International Journal of Earth Sciences (2023) 112:1613–1634
https://doi.org/10.1007/s00531-023-02318-1

ORIGINAL PAPER

Faulting, basin formation and orogenic arcuation at the Dinaric–Hellenic junction (northern Albania and Kosovo)

Marc U. Grund[1] · Mark R. Handy[1] · Jörg Giese[2,3] · Lorenzo Gemignani[1] · Jan Pleuger[1] · Kujtim Onuzi[4]

Received: 19 April 2022 / Accepted: 3 May 2023 / Published online: 17 July 2023

Abstract

The Dinaric–Hellenic mountain belt bends where two fault systems transect the orogen: (1) the dextral Shkoder-Peja Transfer Zone (SPTZ), active sometime between the Late Cretaceous and middle Eocene; (2) the Shkoder-Peja Normal Fault (SPNF), which accommodated NW–SE directed orogen-parallel extension. The SPTZ dextrally offsets the Dinaric–Hellenic nappes by ~ 75 km, a displacement attributed to reactivation of an Early Mesozoic rift transfer zone in the Adriatic margin during Paleogene subduction of the Pindos Ocean. This subduction involved an initial counter-clockwise rotation of the Hellenides with respect to the Dinarides around a pole at the NW end of the Budva–Krasta–Cukali–Pindos Basin. The SPNF overprints the SPTZ and is a composite structure comprising five fault segments: four of them (Cukali–Tropoja, Decani, Rožaje, Istog) were active under ductile-to-brittle conditions. They downthrow the West Vardar Ophiolite in the hanging wall. The Cukali–Tropoja and Decani segments exhume domes with anchizonal-to-greenschist-facies metamorphism in their footwalls. These structures formed during a first-phase of extension and clockwise rotation, whose Paleocene age is constrained by cross-cutting relationships. A second extensional phase was accommodated mainly by the fifth (Dukagjini) segment of the SPNF, a subsurface normal fault bordering syn-rift, mid-late Miocene clastic and lacustrine sediments in the Dukagjini Basin (DB) that are sealed by Plio-Pleistocene strata. This later phase involved subsidence of Neogene basins at the Dinaric–Hellenic junction coupled with accelerated clockwise oroclinal bending. The driving force for clockwise rotation is thought to be bending and rollback of the untorn part of the Adriatic slab beneath the Hellenides.

Keywords Dinarides · Hellenides · Orogenic arcuation · Neogene basins · Oroclines

Introduction

Orogenic arcs, also called oroclinal bends or oroclines (Marshak 1988; Rosenbaum 2014), are a first-order feature of the Alpine-Mediterranean mountain belt (Rosenbaum and Lister 2004, Fig. 1a). These range from the tight loops of the Western Alps, Carpathians and Calabria, to open bends, for example, along the Dinarides and Hellenides that border the Adriatic plate (Fig. 1a). What distinguishes the latter from the aforementioned loops is that it coincides with an orogen-parallel change in the mode of Neogene plate convergence, from retreating subduction, collision and slab bending in the Hellenides (Hollenstein et al. 2008; Kahle et al. 2000; Royden and Papanikolaou 2011) to oblique dextral collision and slab tearing in the Dinarides (Wortel and Spakman 2000; Rosenbaum and Lister 2004; Handy et al. 2019). In this paper, we use the term "Dinaric–Hellenic Junction" to refer to the segment of the orogen at the borders of Albania, Montenegro, and Kosovo marked by an oroclinal bend of about 30° (Fig. 1b). We purposefully avoid the expression "Albanides" sometimes used for this segment (Cvijić 1901; von Nopcsa 1905; Meço and Aliaj 2000), because the general sequence of Late Cretaceous–Paleogene nappes is the same along the chain in the southeastern Dinarides and northwestern Hellenides (Schmid et al. 2020). The nappes beneath the West Vardar Ophiolite on either side of the SPNF comprise sheets of late Paleozoic basement, Mesozoic

✉ Marc U. Grund
m.grund@fu-berlin.de

[1] Institut für Geologische Wissenschaften, Freie Universität Berlin, Deutschland, Germany

[2] Geological Survey of Norway, NGU, Trondheim, Norway

[3] Present Address: Bundesanstalt für Geowissenschaften und Rohstoffe (BGR), Hannover, Germany

[4] Institute of Geosciences, Polytechnic University of Tirana, Tiranë, Albania

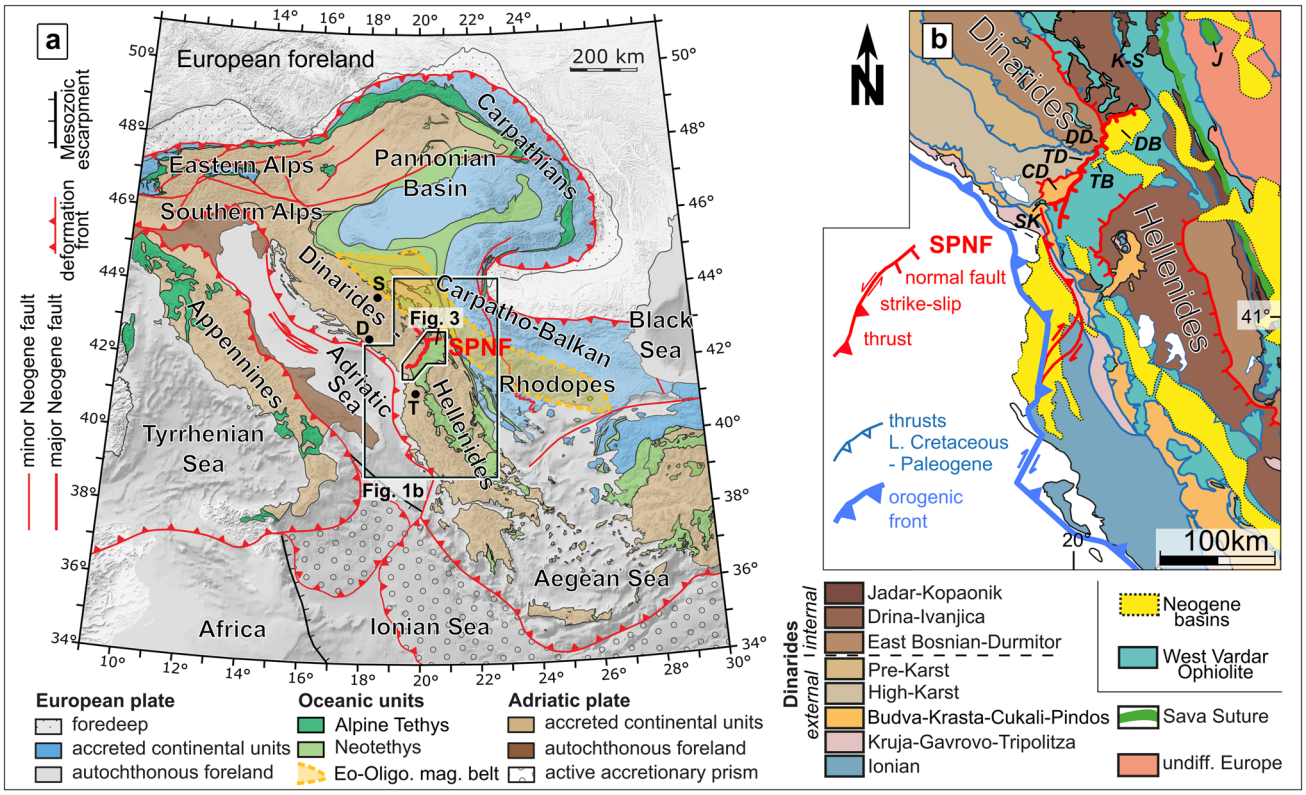

Fig. 1 **a** Alpine orogens of the central Mediterranean and their accreted European (blue) and Adriatic (brown) crust. Boxed areas show locations of Figs. 1b and 3. Belt of Eocene–Oligocene magmatism (pale orange) compiled from Handy et al. (2015, their Fig. 3). Cities: *D* Dubrovnik, *S* Sarajevo, *T* Tirana. **b** Dinaric–Hellenic junction with SPNF system (thick red line) and the associated structures: *SK* Shkoder Klippe, *CD* Cukali Dome, *TB* Tropoja Basin, *TD* Tropoja Dome, *DD* Decani Dome, *DB* Dukagjini Basin. *K-S* Kopaonik and Studenica core-complexes with Oligo-Miocene intrusions and in the southern Dinarides as compiled from Schefer et al. (2011), *J* Jastrebac core-complex (Marović et al. 2007). Nappes, Neogene basins, orogenic front, thrusts and normal faults modified from Schmid et al. (2020, 2008)

platform carbonates and Paleogene flysch derived from the early Mesozoic Adriatic continental margin (Louis 1927; Babić et al. 2002; Gawlick et al. 2008; Schmid et al. 2008; Bortolotti et al. 2013; Scherreiks et al. 2014).

Orogenic bending at the Dinaric–Hellenic junction reaches back to pre-Neogene time, as revealed by paleomagnetic studies indicating block rotation since the Late Cretaceous (Kissel et al. 1995; Márton et al. 2003, 2014). Metamorphic core complexes in the internal Dinarides (Fig. 1b) document post-nappe extension in late Paleogene time (Schefer et al. 2011; Schefer 2012; Stojadinovic et al. 2013, 2016; Mladenović et al. 2015; Erak et al. 2016). This was roughly coeval with subduction of an arm of the Neotethyan Ocean, relics of which are preserved in the Hellenic Nappes (Pindos unit) and equivalent units in the Dinarides (Krasta-Cukali-Pindos unit in Fig. 1b; van Hinsbergen et al. 2020; Schmid et al. 2020, 2008). The relationship of these events to the pre-Neogene component of oroclinal bending is unclear. A main goal of this paper is therefore to examine the spatial–temporal evolution of the faults marking the Dinaric–Hellenic Junction in order to ascertain the causes of bending, and if possible, to determine how orogenic crust responds to along-strike changes in plate convergence.

The clockwise bend of the Dinaric–Hellenic Orogen coincides with a system of normal faults that cut across the NE-dipping Dinaric–Hellenic nappe pile of Late Cretaceous to Paleogene age (faults marked in red in Fig. 1b, e.g., Schmid et al. 2008). The main fault in this system is the Shkoder-Peja* Normal Fault or SPNF (Fig. 1) that juxtaposes the Dinaric nappe stack in its footwall with the structurally highest nappe, the West Vardar Ophiolite, in its hanging wall. The name stems from the cities of Shkoder and Peja, respectively, in northern Albania and western Kosovo located near the ends of this SE-dipping normal fault system.

**Shkodra–Pejë (Albanian), Skadar–Peć (Serbo-Croatian), Scutari-Peć (Italian) or Shkoder-Peja (Albanian-English).*

The SPNF system coincides with the 30° bend of the mountain belt in map view (Fig. 1a), suggesting that this system is associated with orogenic arcuation (van Hinsbergen et al. 2005; Kissel et al. 1995; Speranza et al. 1995). Indeed, Handy et al. (2019) proposed that the fault is not

strictly a normal fault, but accommodated scissor-like motion with top-SE downthrow of the hanging wall block increasing northeastwards away from a vertical rotation pole near Shkoder (Fig. 2). The amount of rotation is poorly constrained in the absence of structural markers and thermochronological studies on either side of the fault. An orogen-parallel change in Mesozoic facies across the SPNF (von Nopcsa 1905; Aubouin and Dercourt 1975) precludes the use of stratigraphy and nappe contacts as markers. The only thermochronological data available so far—zircon U–Th/He, (ZHe) data, and apatite fission-track data, (AFT), (Muceku et al. 2006, 2008) indicate early Pliocene (4-6 Ma) exhumation of ~ 1.2 mm/year (Muceku et al. 2008) and cooling of units further to the SE of the SPNF. This overlaps with the Mio-Pliocene age of syn-extensional sediments in basins discordantly overlying the West Vardar Ophiolites in the hanging wall of the SPNF (marked yellow in Fig. 1b).

Another puzzling feature of the Dinaric–Hellenic Junction is the dextral offset of the West Vardar Ophiolite sheet by some 75 km in map view (Fig. 1). This offset gave rise to the idea of the "transversale de Scutari-Peć" (Aubouin and Dercourt 1975) or Shkoder-Peja Transverse Zone (SPTZ, Handy et al. 2019) which is truncated by, and therefore, older than, the SPNF. Three structural domes in the footwall of the SPNF (Cukali, Tropoja and Decani Domes, Figs. 1b and 3) deform and therefore post-date the Dinaric nappe stack, but their kinematic relationship to the SPTZ and SPNF is enigmatic. It is tempting to relate doming to footwall exhumation along the SPNF (Handy et al. 2019), but the domes affect different levels of the nappe stack, suggesting varied amounts and ages of exhumation along the SPNF.

The hanging wall of the SPNF contains several Neogene fresh-water basins (Neubauer et al. 2015; Gemignani et al. 2022), the largest of which is the Dukagjini Basin (DB; Figs. 1b and 3), also termed the Metohija Basin (Elsie 2004; Elezaj 2009; Handy et al. 2019) or Western Kosovo Basin (Gemignani et al. 2022). Middle Miocene clastics in this basin (Elezaj 2009; Elezaj and Kodra 2012) have been used to date downthrow of the hanging wall of the SPNF (Handy et al. 2019), but the Plio-Pleistocene strata (Knobloch et al. 2006; Legler et al. 2006; Elezaj 2009; Elezaj and Kodra 2012) are not visibly in contact with surface exposures of

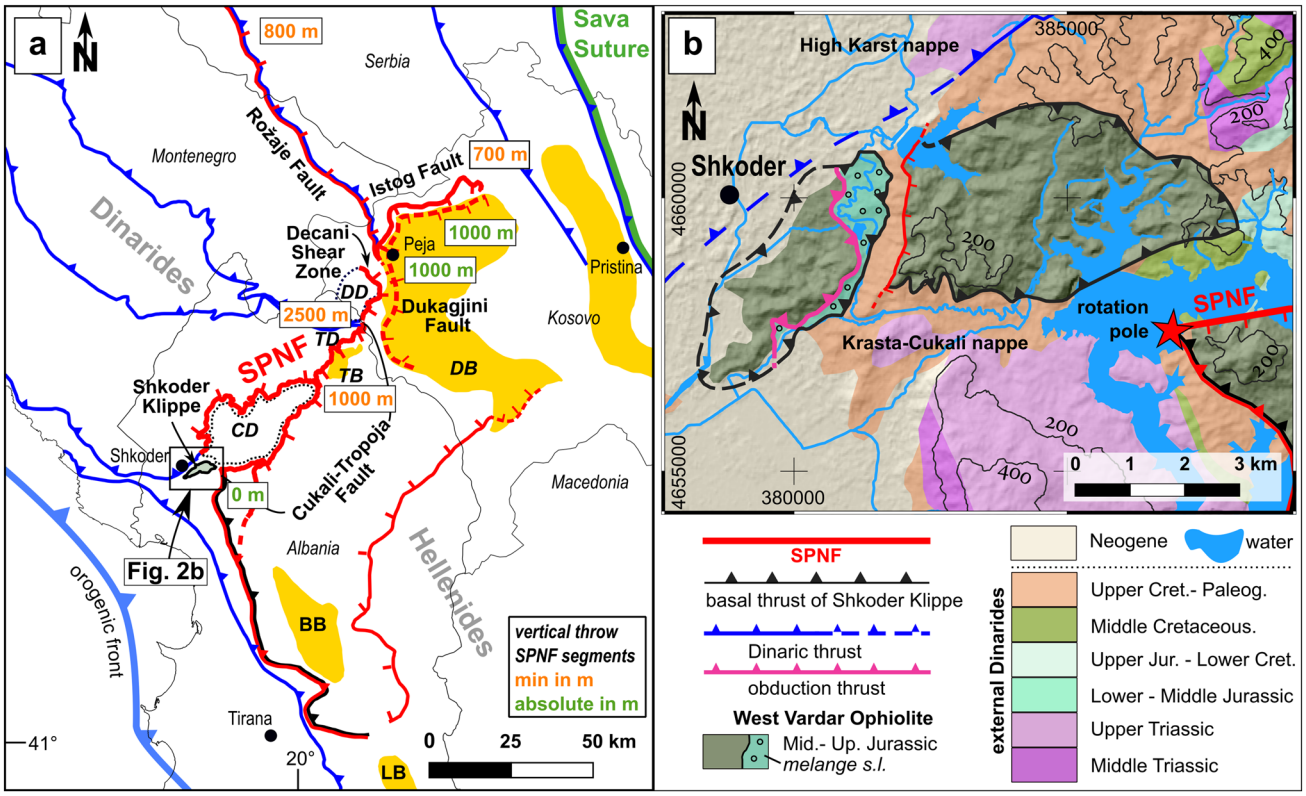

Fig. 2 Faults at the Dinaric–Hellenic junction: **a** SPNF system (thick red line), Dinaric thrusts (dark blue) and present orogenic front (pale blue). *SV* Sava Suture, dashed red lines represent subsurface faults, chiefly the Dukagjini Fault beneath in the Dukagjini Basin (DB). Neogene basins in yellow: *TB* Tropoja basin, *BB* Burrel Basin, *LB* Librazhd Basin. Major structures in the footwall of the SPNF: Cukali Dome (CD), Tropoja Dome (TD) and Decani Dome (DD). Box indicates location of **b** Shkoder Klippe near city of Shkoder in northern Albania. SPNF rotation pole from Handy et al. (2019). Tectonic units from Schmid et al. (2020, 2008). Hillshade model and contour lines in **a** are extracted from ASTER GDEM (Abrams et al. 2020). Map in **b** is simplified from Groß et al. (2014)

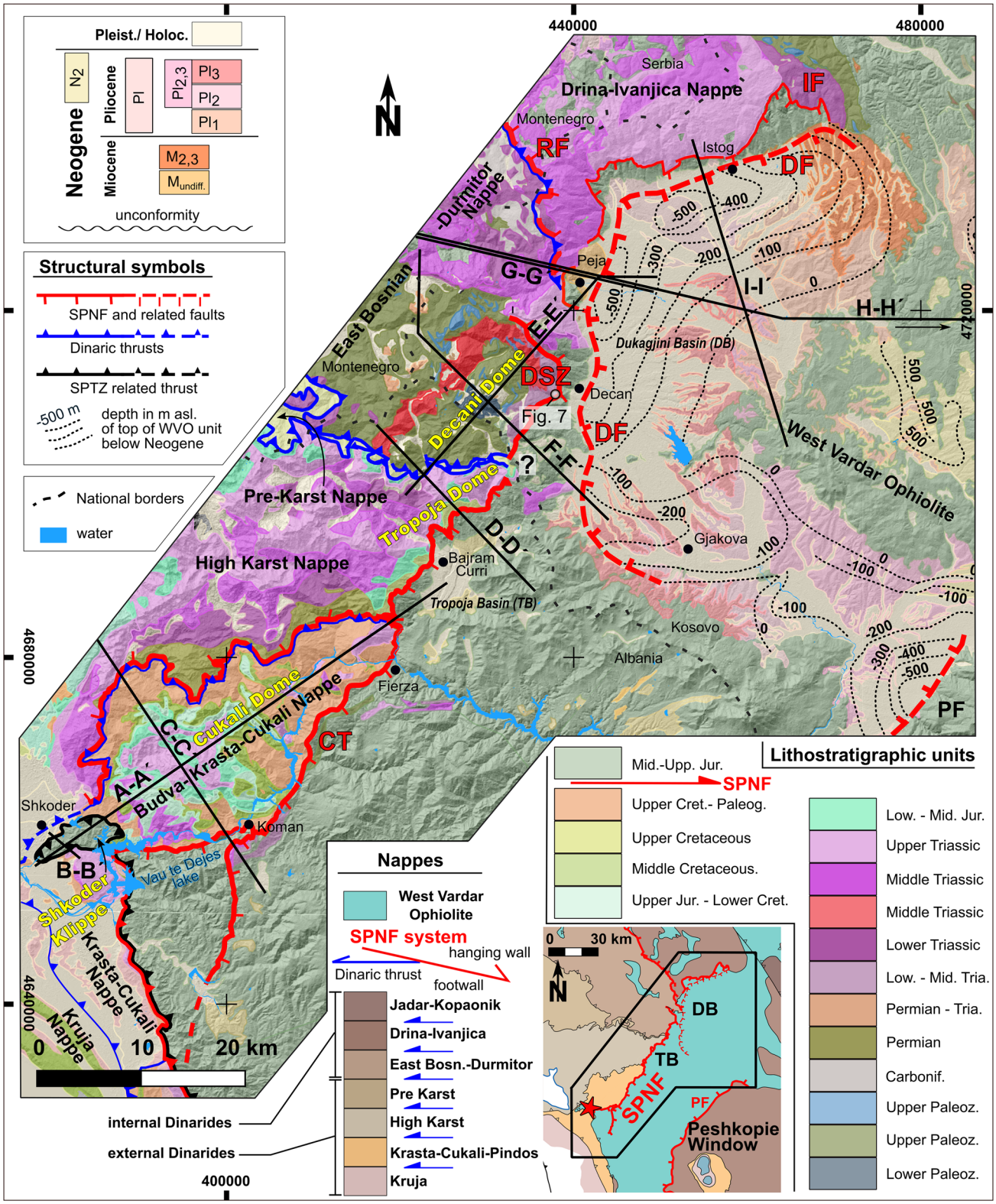

the SPNF mapped so far. Either the SPNF comprises several coeval branches, or these faults formed at different times in close proximity.

Finally, the Dinaric–Hellenic Junction coincides with changes in the depth and orientation of positive P-wave anomalies in the mantle, with a short Dinaric slab anomaly north of the junction contrasting with a longer slab anomaly

◂**Fig. 3** Geological map of the Dinaric–Hellenic Junction. Profiles A-A´ to I-I´ shown in Figs. 4, 6 and 9. Bold red letters refer to segments of the SPNF: *CT* Cukali–Tropoja Fault, *DSZ* Decani Shear Zone, *DF* Dukagjini Fault, *RF* Rožaje Fault, *IF* Istog Fault. Bold black letters: *PF* Prizren-Vranica Fault. Inset map, *TB* Tropoja Basin, *DB* Dukagjini Basin. Red star marks vertical rotation pole of the SPNF system (Handy et al. 2019). Nappe structure after Schmid et al. (2008 and 2020). Lithological units adopted from the national geological maps of Albania (1:200,000 and 1:50,000, Xhomo et al. 2002) and ex-Yugoslavia, maps: K 34–53 "Pec", K34-65 "Kukes" (*Osnovna Geološka Karta SFRJ, 1:100.000* 1966–1977, Antonijević 1969). Note that the West Vardar Ophiolite is modified from the ex-Yugoslavian map to includes a basal mélange with fragments of the underlying Dinaric nappes. Depth to basement in the DB taken from the Tectonic Map of Kosovo 1:200.000 (Legler et al. 2006). CRS of map: WGS 84, UTM zone 34N, DEM based on ASTER GDEM (Abrams et al. 2020)

in the south that trends north–south (Bijwaard and Spakman 2000; Handy et al. 2019). Debate centres on the causes of this subcrustal change in structure and its relationship to structures at the surface. Handy et al. (2019) proposed that tearing or breakoff of the Dinaric part of the slab (Wortel and Spakman 2000) lead to faster rollback of the longer, untorn Hellenic segment. Nucleation of the SPNF then facilitated orogenic arcuation. Geodetic studies show that ongoing arcuation and orogen-parallel extension of the Hellenides is limited to the north by the SPNF system (e.g. D'Agostino et al. 2020; Jouanne et al. 2012), suggesting that this system is still accommodating arcuation today. Another goal of this paper is, therefore, to clarify the relationship of fault kinematics to patterns of doming, exhumation and basin subsidence at the surface and to subduction of lithosphere at depth.

This study presents structural and kinematic evidence that today`s bend in the Dinaric–Hellenic chain is a long-lived, partly pre-Neogene feature that nucleated along an inherited rift transfer within the Adriatic margin. In the next chapters, we introduce key features of the Dinaric–Hellenic Junction as a prelude to new field evidence that the SPNF is a composite structure comprising several distinct, differently aged segments. We discuss how these segments accommodated varied amounts of orogen-normal and parallel extension, doming, as well as why Neogene sedimentary basins can be attributed to activity of primarily one segment of the SPNF. We provide age constraints as a basis for a new conceptual model of faulting and basin formation. In contrast to Handy et al. (2019), it is argued that strike-slip activity of the SPTZ was associated with minor oroclinal bending and possible local extension during differential shortening of the Dinarides and Hellenides in Late Cretaceous time. Most clockwise bending was accommodated later by two phases of normal faulting on the SPNF, the first during late Paleogene detachment and retreat of the Adriatic slab and the second during Neogene rollback subduction of Neotethys (Handy et al. 2019), part of the Greater Adria plate (van Hinsbergen et al. 2020).

Structure and history of the Dinaric–Hellenic nappes

The highest unit in the nappe pile, the West Vardar Ophiolite, is the only reliable structural marker for the SPNF and SPTZ faults, being dextrally offset along the SPTZ and vertically downthrown to the SE along the SPNF (Schmid et al. 2008; Handy et al. 2019). We follow geochemical, structural and stratigraphic arguments supporting the idea that the Neotethyan ophiolite belts of the Dinarides and northern Hellenides, including the West Vardar Ophiolite, originated from a single, oceanic basin (Bortolotti et al. 2004, 2013; Schmid et al. 2008) of Early-Middle Jurassic age (Halamić et al. 1999; Liati et al. 2004; Ozsvárt et al. 2012; Lugović et al. 2015). The West Vardar Ophiolite was obducted SW-ward onto the Adriatic passive margin of Early-Middle Triassic age (Ferrière et al. 2016; Gawlick et al. 2008; Haas et al. 2019; Halamić et al. 1999; Sudar et al. 2013) in Late Jurassic to Early Cretaceous time (Pamić 2002; Scherreiks et al. 2014; Tremblay et al. 2015) as documented by Ar–Ar amphibole ages from its metamorphic sole (Dimo-Lahitte et al. 2001; Borojević Šoštarić et al. 2014) and biostratigraphic ages in its sub-ophiolitic mélange (Vishnevskaya et al. 2009). The internal Dinaric nappes (Schmid et al. 2008, 2020) underlying the West Vardar Ophiolite and derived from the Adriatic passive margin (Fig. 3, Jadar–Kopaonik, Drina–Ivanjica–Korab = Upper Pelagonian nappe, East Bosnian–Durmitor = Lower Pelagonian nappe) were subsequently imbricated with the obducted West Vardar Ophiolite sheet during SW-directed Dinaric thrusting in Paleogene time (Schmid et al. 2020). Collision initiated in Late Cretaceous time with closure of the part of Neotethys that separated Adria and Europe (Sava Suture in Figs. 1 and 2, Dimitrijević 1997; van Hinsbergen et al. 2020; Schmid et al. 2008, their Fig. 5h). Dinaric thrusting continued until Early Oligocene time in the external nappes of the Dinarides (Pre-Karst, High Karst, Krasta–Cukali, Kruja and Ionian nappes in Fig. 3; Xhomo et al. 2002; Tari 2002; Schmid et al. 2008)) as constrained by the youngest biostratigraphic age of flysch underlying the basal thrust of each nappe. These nappes are deformed by the aforementioned Cukali, Tropoja and Decani Domes in the footwall of the SPNF (Figs. 3 and 4). Also in the footwall of the SPNF near Shkoder is a small klippe of West Vardar Ophiolite that directly overlies Eocene flysch of the Krasta–Cukali nappe (Figs. 2, 3 and 4). This klippe, the Shkoder Klippe, is significant in the following chapters for determining strike-slip motion on the SPTZ.

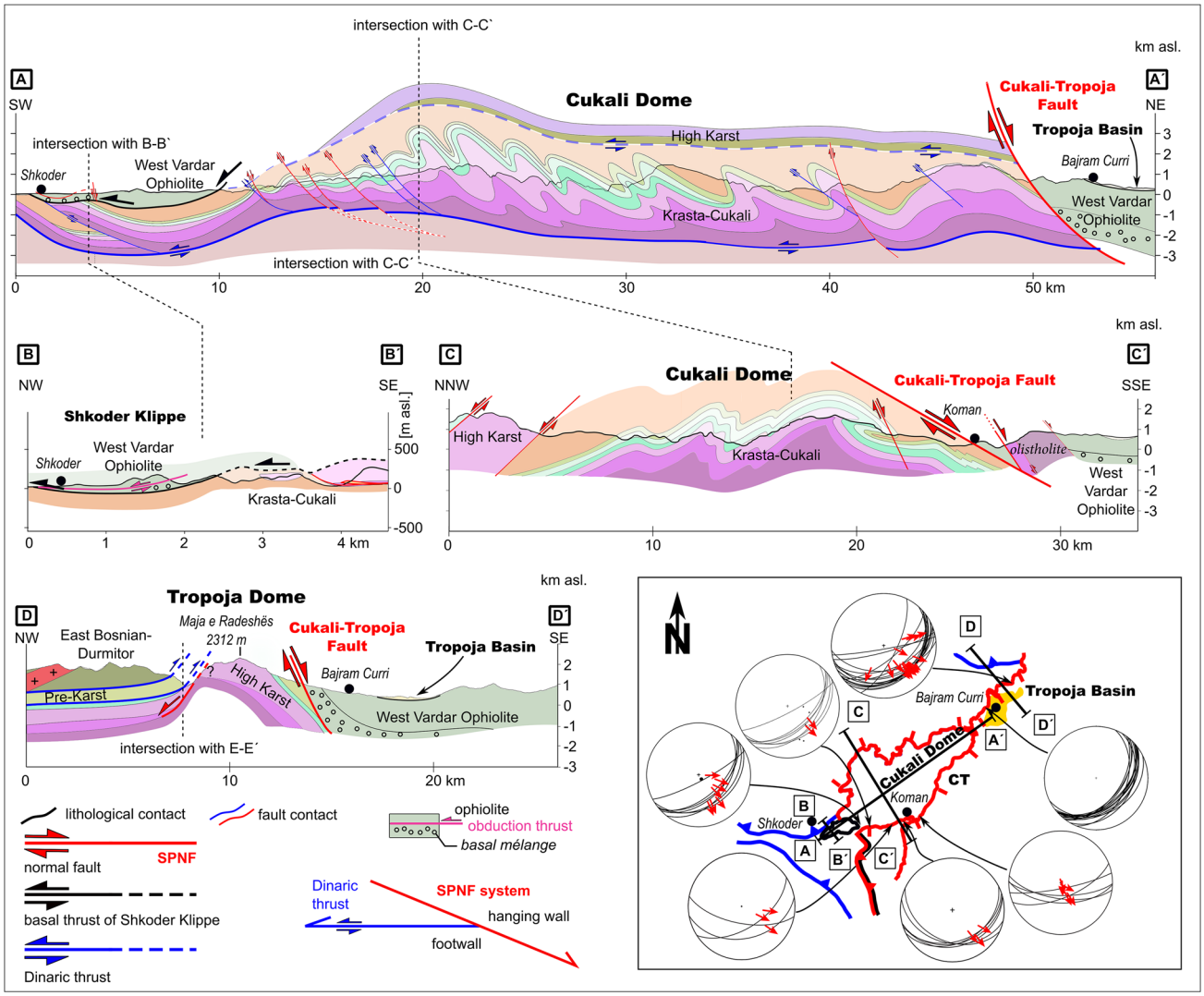

Fig. 4 Profiles along and across the Cukali–Tropoja Fault, including the Shkoder Klippe, Cukali Dome and Tropoja Dome. Location of profile traces shown in Fig. 3. No vertical exaggeration. Topography extracted from ASTER GDEM (Abrams et al. 2020). Lower-hemisphere equal-area projections shows orientation of fault surfaces (black lines) and striations (red arrows) with arrows indicating motion of hanging wall. Geology based on maps K 34–53 "Pec", K34-65 "Kukes" (*Osnovna Geološka Karta SFRJ, 1:100.000* 1966–1977, Antonijević 1969) and Geological Map of Albania 1:200,000 and 1:50,000 (Xhomo et al. 2002)

The Hellenic Nappes south of the SPTZ and SPNF have the same basic structure as the Dinaric Nappes, except that the Krasta–Cukali Nappe is exposed in a tectonic window (Peshkopie Window, Fig. 3, inset map) surrounded by the overlying Upper Pelagonian Nappe in addition to occuring along the NE-dipping thrust front. North of the Peshkopie Window a SSW-NNE striking normal fault downthrows the West Vardar Ophiolite to the NE in the hanging wall (Figs. 1b and 2a). The NE end of this fault (Prizren-Vranica Fault, *PF* in Fig. 3) is sealed by Pleistocene sediments and is interpreted as conjugate to the SPNF system (Handy et al. 2019; their Fig. 13e). In the Hellenides, the West Vardar Ophiolite directly overlies the external nappes (Krasta-Cukali and Kruja Nappes). The Krasta-Cukali Nappe with its Early Jurassic pelagic strata (Robertson and Shallo 2000; Schmid et al. 2020; Fig. 3) is the along-strike equivalent of the Pindos Nappe in the central Hellenides, which contains ophiolites of the Pindos Basin (Shallo and Dilek 2007; Rassios and Dilek 2009; Robertson et al. 2009). This along-strike correlation has important implications for constraining transverse motion of the SPTZ, as discussed below.

Two points regarding the Dinaric–Hellenic nappe structure have direct bearing on the structure of the SPTZ and SPNF: first, the widely accepted theory of a single-ocean origin for the imbricated West Vardar

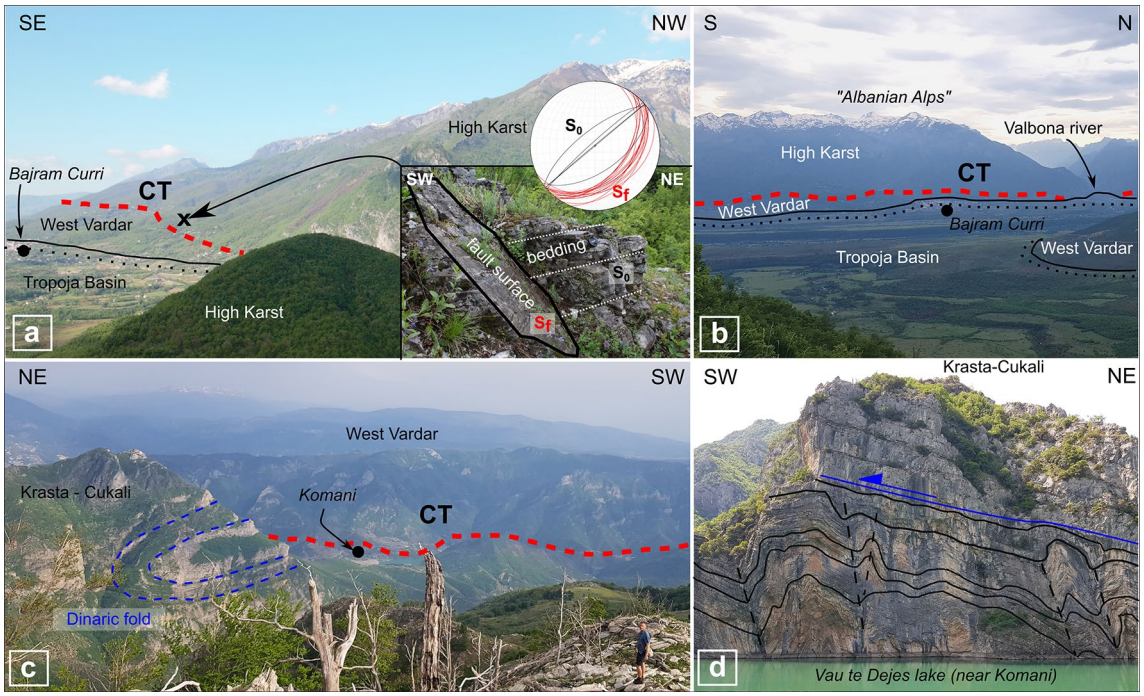

Fig. 5 View of the Tropoja Basin (**a**, **b**) and the Cukali Dome (**c**, **d**). Bold red dashed lines in all plates indicate trace of the Cukali–Tropoja Fault (CT) segment of the SPNF. **a** The SPNF juxtaposes the High Karst Nappe (footwall) with the West Vardar Ophiolite (hanging wall) which is unconformably overlain by Plio-Pleistocene sediments of the Tropoja Basin (line with dots). The gorge beyond the hill in the foreground is the entrance to the Valbona Valley, where Pleistocene river terraces (lower left) and Holocene carbonate breccia (at entrance to the Valbona valley) seal the SPNF fault. Lower hemisphere equal-area projection shows orientation of bedding (S_0, black great circles) and fault surfaces (S_f, red great circles) in massive and thinly-bedded limestone of the High Karst Nappe; **b** View across the Tropoja Basin (foreground) of the West Vardar Ophiolite and High Karst Nappe, respectively, in the foot- and hanging wall of the Cukali–Tropoja Fault. The topographic relief across the fault measured from the basin surface to the highest peaks of the Albanian Alps is ~ 2500 m. Note the flat landscape with river terraces in the foreground incised in horizontal Plio-Pleistocene sediments unconformably overlying the West Vardar Ophiolite; **c** View from top of Mount Cukali showing a large SW-vergent Dinaric fold. **d** Dinaric folds and thrust of Cretaceous carbonate of the Krasta–Cukali Nappe at the Vau te Dejes reservoir lake near Komani (location of lake in Figs. 2 and 3)

Ophiolite (e.g., Schmid et al. 2008, 2020; Bortolotti et al. 2013) enables us to use it as a marker for dextral offset along the SPTZ of ~ 75 km (Handy et al. 2019; Schmid et al. 2020). An older multi-ocean hypothesis for this ophiolite body (e.g. Karamata 2006; Robertson and Shallo 2000) has been disproved on both structural and geochemical grounds (Carosi et al. 1996; Schmid et al. 2008, 2020; Bortolotti et al. 2013). Second, the SPNF does not cut the entire Dinaric nappe pile, but ends in the NE and SW, respectively, in the Drina–Ivanjica–Korab and Krasta–Cukali Nappes (Fig. 3, inset). The SW end of the SPNF near Shkoder becomes a NW–SE trending thrust within flysch of the Krasta–Cukali nappe, where it accommodated SW-directed, Neogene-to-Present imbrication of the older Paleogene nappe pile (Handy et al. 2019).

Structure and kinematics

Segments of the SPNF

The SPNF is a system of SE- to E-dipping normal faults with five segments (Figs. 2 and 3) that are kinematically related, even though they are not all continuous and of the same age: (1) The Cukali–Tropoja Fault bordering the Cukali- and Tropoja Domes in its footwall (labelled CD and TD in Fig. 2a) and extending northwest to the Plio-Pleistocene Tropoja Basin in its hanging wall near the Albanian town of Bajram Curri; (2) The Decani Shear Zone juxtaposing the Decani Dome in its footwall (DD in Fig. 2a) with the West Vardar Ophiolite in its hanging wall; (3) The Rožaje Fault running along the thrust of the Drina–Ivanjica Nappe in its hanging wall and the East Bosnian–Durmitor Nappe in its footwall; (4) The Istog

Fault skirting the western and northern parts of the DB (labelled DB in Fig. 2a) and juxtaposing sub-ophiolitic mélange of the West Vardar Ophiolite in its hanging wall with the Drina–Ivanjica Nappe in its footwall; (5) The Dukagjini Fault, a subsurface fault buried beneath the Plio-Pleistocene cover of the DB and located in the hanging wall of the Decani Shear Zone, the Rožaje Fault and Istog Fault. These segments cut progressively higher units of the NE-dipping Dinaric nappe stack going from SW to NE.

(1.) The Cukali–Tropoja Fault forms the southeastern border of the Cukali Dome (Figs. 3 and 4). The northern limb of the dome is bounded by a NW-dipping normal fault that is conjugate to the SPNF. The Cukali–Tropoja Fault forms the SE limit of the Cukali Dome and truncates SW-directed thrusts and folds of the Krasta–Cukali and High Karst Nappes within this dome. The fault itself comprises a cataclastic zone up to 3 m thick that is gradational in its footwall to chlorite-sericite-bearing mylonite derived from the clay- and silt-rich shales and slates of the Late Cretaceous-Eocene Krasta–Cukali flysch and Late Cretaceous marl of the High Karst nappe. This mineral assemblage is consistent with faulting under lower greenschist facies to anchizonal conditions. The ductile style of the post-nappe folds and the occurrence of fine-grained dynamic recrystallization in mylonitic limestone indicate a temperature of at least 250 ℃ (e.g., Ferrill et al. 2004) in the footwall of the Cukali–Tropoja Fault prior its activity (Handy et al. 2019, their Fig. 4c). Within about 100 m of the fault plane, the SE-dipping bedding and schistosity in the footwall steepen into concordance with the brittle fault plane, which is locally coated with talc, serpentine and calcite. Serpentine is derived exclusively from the overlying West Vardar Ophiolite and its sub-ophiolitic mélange in the hanging wall. The drag of the schistosity in the footwall units indicates top-SE motion of the hanging wall block (Handy et al. 2019, their Fig. 4b). This is consistent with the sense of shear determined from slickenfibres on fault planes dipping ~ 25° SE (Fig. 4 inset map, Groß et al. 2014, Fig. 5a, Handy et al. 2019, their Fig. 3).

The SW end of the Cukali–Tropoja Fault roots in Paleogene flysch of the Krasta–Cukali nappe near the Vau te Dejes reservoir lake (Figs. 2b, 3 and 5d) near Shkoder (star in Fig. 2b) and continues southward as a W- to SW-directed Miocene thrust along the mountain range bordering the Peri-Adriatic foredeep basin (Figs. 2b and 3; Handy et al. 2019). This thrust is also joined by the main N-S trending branch of the SPNF that cuts into the West Vardar Ophiolite near the town of Koman (Fig. 3).

The NE end of the Cukali–Tropoja Fault with the Tropoja Dome (Fig. 4) in its footwall skirts the Plio-Pleistocene Tropoja Basin (Figs. 3, 5a and 5b) and coincides with the boundary between red shales of the sub-ophiolitic mélange and Late Cretaceous marly shale of the High Karst nappe (Fig. 3). The Cukali and Tropoja Domes plunge to the NE and are truncated by the Cukali–Tropoja Fault (Fig. 4, profiles A-A´, and D-D', Figs. 10a, d). The northern limb of the Cukali Dome comprises thinned and excised Middle Triassic strata, marking a NE-dipping normal fault that is conjugate to the Cukali–Tropoja Fault (Fig. 4, profile D-D´). The topographic relief in its footwall increases markedly along strike (~ 1000 m in Fig. 4, profile A-A´, > 2000 m near Fierza in Fig. 5c to ≥ 2500 m near Tropoja, Fig. 5b), as reflected by the contrasting morphology of platform carbonates and ophiolite units, respectively, in the foot- and hanging walls (Handy et al. 2019, their Fig. 4a; Gemignani et al. 2022, their Fig. 4).

Using this topography as a crude structural marker, one can estimate a throw ranging from 0 near Shkoder to a minimum of ~ 2500 m at the Tropoja Basin (Fig. 2a and Fig. 5b). The latter was obtained from the difference in altitude of lowest (200–250 m asl, Valbona river bed) and highest (Jezerca peak 2694 m) exposures of High Karst nappe in the footwall of the fault. This is much less than the 7 km of maximum throw estimated by Handy et al. (2019) for the same locality, obtained by projecting the base of the West Vardar Ophiolite from N to S over several tens of km along strike into the section.

(2.) The Decani Shear Zone is a ~ 1 km wide zone (Fig. 6, profiles E-E´ and F-F´, Fig. 7) of mylonitic limestone and siliciclastic schist that dip E to ESE. The protoliths affected by shearing are Mesozoic carbonates and locally breccious Triassic carbonates of the East Bosnian–Durmitor nappe and shales and slates of the sub-ophiolitic mélange of the West Vardar Ophiolite, respectively, in the foot- and hanging walls (Fig. 7). Though this shear zone appears to be continuous along strike with the Cukali–Tropoja Fault (Fig. 3), it differs from the latter in being thick and pervasively mylonitic, with only subordinate, overprinting brittle deformation.

The mylonite comprises sericite-chlorite-bearing schist without biotite, and carbonates with dynamically recrystallized calcite (Fig. 7b–d). These features indicate temperatures between 300 and 350 °C, typical of lower greenschist-facies conditions (Okrusch and Matthes 2009; Philpotts and Ague 2009). Temperature estimates for marble-bearing shear zones (Thassos Island, Greece) similar to the mylonitic marbles of the Decani Shear Zone indicate syntectonic temperatures of 300–350 °C (Bestmann et al. 2000).

The mylonite derived from bedded limestone and shale protoliths contains moderately E- to ESE-dipping (30–60°, Fig. 7- profile) shear bands on the cm, m- and multi-meter scales, as well as slickenfibres that mostly indicate top-down-to-the-E motion of the hanging wall.

The southern end of the Decani Shear Zone truncates the thrust of the East Bosnian–Durmitor Nappe onto the Pre-Karst Nappe. As an aside, we were unable to visit the actual

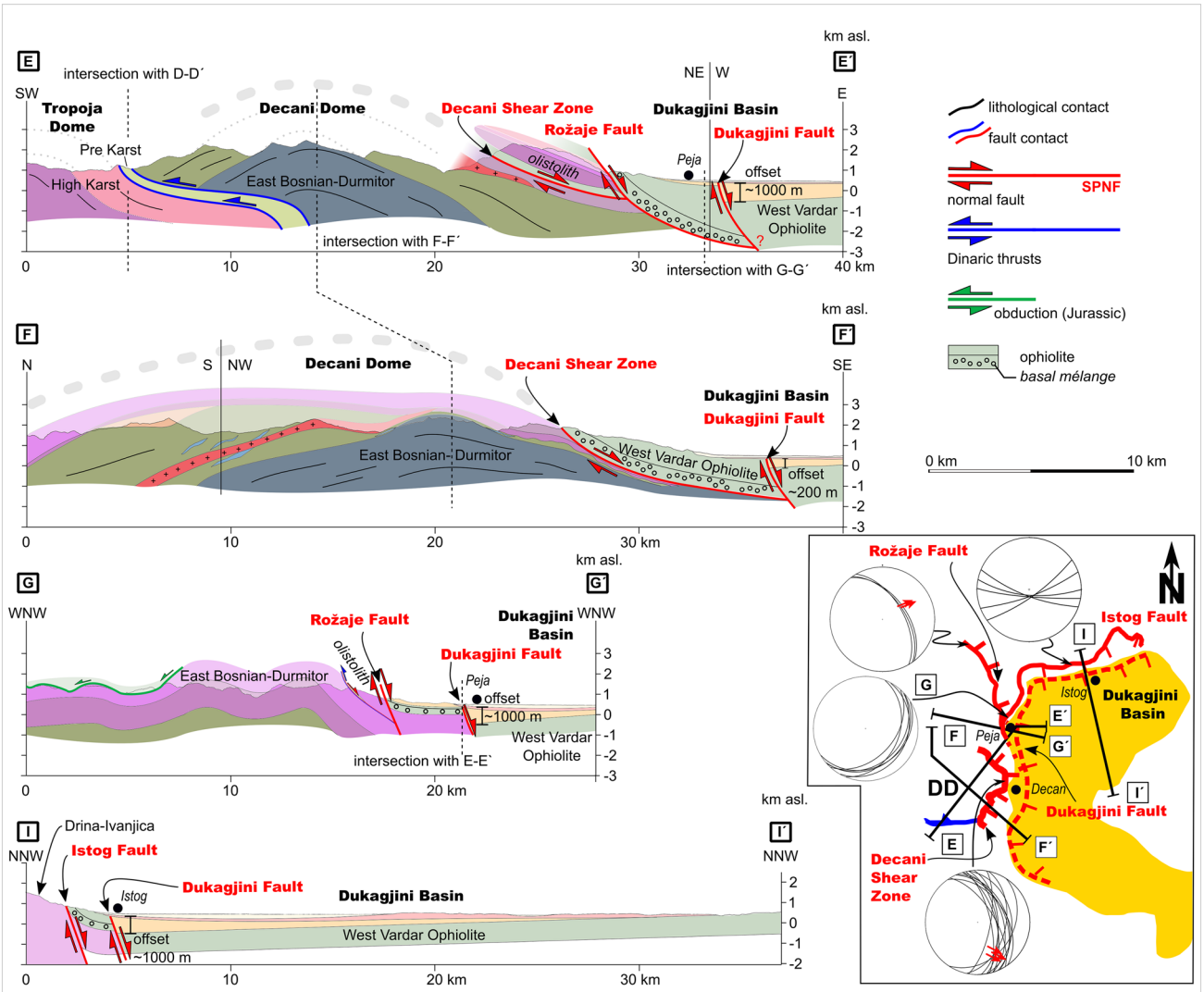

Fig. 6 Profiles of the Decani Shear Zone, Decani Dome, Rožaje Fault and Dukagjini Fault along the western and northwestern sides of the Dukagjini Basin. Location of profile traces shown in Fig. 3. No vertical exaggeration. Inset map: *DD* Decani Dome; lower hemisphere equal-area projections show orientation of fault surfaces and striations (black great circles and red arrows, respectively), with arrow heads indicating motion of the hanging wall. Topographic profiles from ASTER GDEM (Abrams et al. 2020). Geology based on maps K 34–53 "Pec", K34-65 "Kukes" (*Osnovna Geološka Karta SFRJ, 1:100.000* 1966–1977, Antonijević 1969) and Geological Map of Albania 1:200,000 and 1:50,000 (Xhomo et al. 2002)

point of truncation (question mark in Fig. 3) at the national border between Kosovo and Albania due to the danger of landmines from the Balkan War in 1995. The shear zone forms the eastern perimeter of the Decani Dome. At the northern limit of this dome, the shear zone steepens and follows the lithological contact between Paleozoic metasediments and Triassic platform carbonates within the East Bosnian–Durmitor Nappe. The Decani Dome exposes pre-Mesozoic metamorphosed basement rocks in its core that are similar to metamorphosed Upper Triassic meta-limestones of the Jadar–Kopaonik Nappe (Fig. 1b, Sudar and Kovács 2006) that indicate peak temperatures of ~ 400–500 ℃ (Sudar and Kovács 2006). The amplitude of the Decani Dome is greatest at its eastern end and decreases both to the N, where the mylonitic foliation of the Decani Shear Zone disappears, and to the S at its junction with the aforementioned thrust of the East Bosnian–Durmitor Nappe onto the Pre-Karst Nappe. These structural relations show that the Decani Dome is asymmetrical, with a steeper eastern limb that has been dragged into concordance with the mylonitic foliation of the E-dipping Decani Shear Zone (Fig. 6, profiles E-E' and F-F', and Fig. 7).

(3.) The Rožaje Fault strikes NNW-SSE. At its southern end near the town of Peja (Fig. 3), the fault is inferred from the absence of a slice of West Vardar Ophiolite exposed along strike to the north, which is interpreted to have been

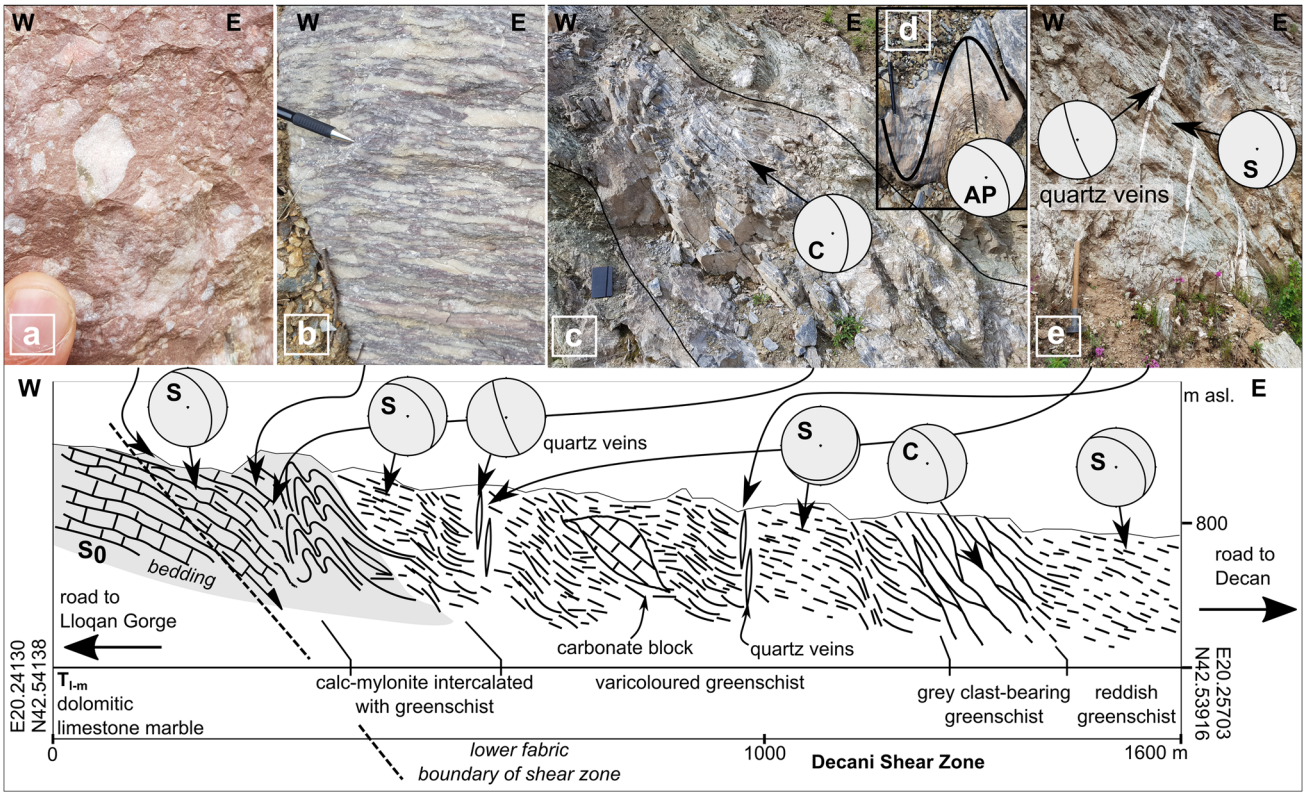

Fig. 7 Road cut of the Decani Shear Zone about 3 km west of the town of Decan (location in Fig. 3; coordinates in WGS 84 (World Geodetic System of 1984, GEM 10C/ EPSG:4326) with outcrops (**a**–**d**) across the lithological boundary between the East Bosnian–Durmitor nappe (footwall, grey) and basal mélange of the West Vardar (hanging wall, white). Dashed line on the left side of the profile marks the lower fabric boundary of the Decani Shear Zone within the East-Bosnian–Durmitor nappe. The Decani overprint is strongest in mylonitic foliation domains marked "C", which are zones of highly non-coaxial shear. The angle between S and C foliations is consistent with downthrow of the Decani hanging wall on the E side of the section (see text, Fig. 6). Lower hemisphere equal-area plots show orientations of foliations and en-echelon quartz veins. Field photos: **a** Brecciated lower to middle Triassic dolomitic marble of the East Bosnian–Durmitor Nappe; **b** Mylonitic fabric in lower to middle Triassic dolomitic marble; **c** Isoclinally folded and mylonitized lower to middle Triassic dolomitic marble intercalated with greenschist and calc-schist of the sub-ophiolitic mélange of the West Vardar Ophiolite; **d** Tight-to-similar fold in mylonitized lower to middle Triassic dolomitic marble with axial plane (AP) dipping 57° to the NE (057°); **e** En-échelon quartz-filled extensional veins (oriented 250/83, dip azimuth/dip) cut the S foliation of the shear zone and are interpreted to have formed during the waning stages of top-down-E motion of the hanging wall

tectonically excised. About 20 km north of Peja, close to the Montenegrinian–Kosovarian border (Fig. 3), NW–SE striking fault planes with slickensides indicate top-down-NE movement of Middle Triassic limestone of the Drina-Ivanjica nappe with respect to Lower Triassic limestone and Paleozoic basement of the East-Bosnian–Durmitor nappe (Fig. 2a). The southward continuation of the Rožaje Fault is speculative due to its poor, largely inaccessible exposure in the Rugova Gorge (Bajraktar et al. 2010; Tahirsylaj et al. 2010) west and north of Peja. It is tempting to link it via a putative system of minor faults to a large, NE-dipping normal fault just S of Peja that juxtaposes West Vardar Ophiolite in the hanging wall with Upper Triassic carbonate of the East Bosnian–Durmitor Nappe in its footwall (Fig. 3). There, the normal fault dips ~ 20–40° to the NE and is marked by a ~ 5 m thick cataclastic zone comprising blocky serpentinite. The fault disappears eastwards below Neogene sediments of the DB (Fig. 3), possibly truncating the Decani Shear Zone at depth (Fig. 10c) and connecting with the Dukagjini Fault (Figs. 3, 6, 9). In the absence of structural and stratigraphic markers to determine the amount of vertical throw directly, we use the vertical thickness of West Vardar Ophiolite exposed to the north along the Rožaje Fault between the Drina-Ivanjica and East Bosnian–Durmitor nappes (maps of Schmid et al. 2008, 2020) to estimate a minimum throw of some 800 m (Fig. 2a). Greater pre-orogenic thicknesses of the ophiolite body and/or thinning of the body during Paleogene nappe imbrication would obviously lead to greater estimates of tectonic excision and vertical throw.

(4.) The Istog Fault (*Istok* in Serbo-Croatian) north of the DB generally strikes WSW-ENE and juxtaposes sub-ophiolitic mélange of the West Vardar Ophiolite in its hanging wall with severely jointed Middle Triassic carbonate of the Drina–Ivanjica Nappe in its footwall (Fig. 3, profile I-I` in Fig. 6). It accommodated top-SE motion (striation orientations in Fig. 6) and can be followed west and north along the arcuate strike of the DB towards its NE end. There, the fault is covered by gently dipping Miocene strata and disappears beneath the Pliocene cover. The Istog Fault has a displacement of at least ~ 700 m along the northern part of the DB (Fig. 2a) based on the vertical offset of sub-ophiolitic mélange in its hanging wall and West Vardar Ophiolite in its footwall (Fig. 3 and Fig. 6, profile I-I`). About 10 km north of Peja, where the strike of the Istog Fault changes from N-S to WSW-ENE, the basinward-dipping sub-ophiolitic mélange of the West Vardar Ophiolite is unconformably overlain by Pliocene strata, constraining basinwards tilting in the hanging wall of the Istog Fault to be older than early Pliocene, probably late Miocene (Fig. 3).

(5.) The Dukagjini Fault is a subsurface fault that has so far only been mapped in geo-electric images as an offset of basement rock, taken to be the West Vardar Ophiolite beneath the DB (Appendix: map and geo-electric resistivity cross sections, Geophysical Institute of the Yugoslavia Republic, 1978, provided by Sali Mulaj, Independent Commission for Mines and Minerals, Pristina, Kosovo). The offset amounts to ~ 1000 m across a horizontal distance of ~ 1 km (Figs. 3 and 8, Fig. 6 profiles E-E´, F-F´, G-G and I-I` and Fig. 9 profile H–H`) as shown in previous geological profiles of the basin (Knobloch et al. 2006; Legler et al. 2006; Linder and Perkuhn 2013). In our profiles, we depict the fault as a discrete surface delimiting a half-graben filled with clastics and lacustrine sediments that gradually decrease in thickness to the east away from the fault. There, the Mio-Pliocene sediments of the basin onlap onto the post-obduction Cretaceous limestone above the West Vardar

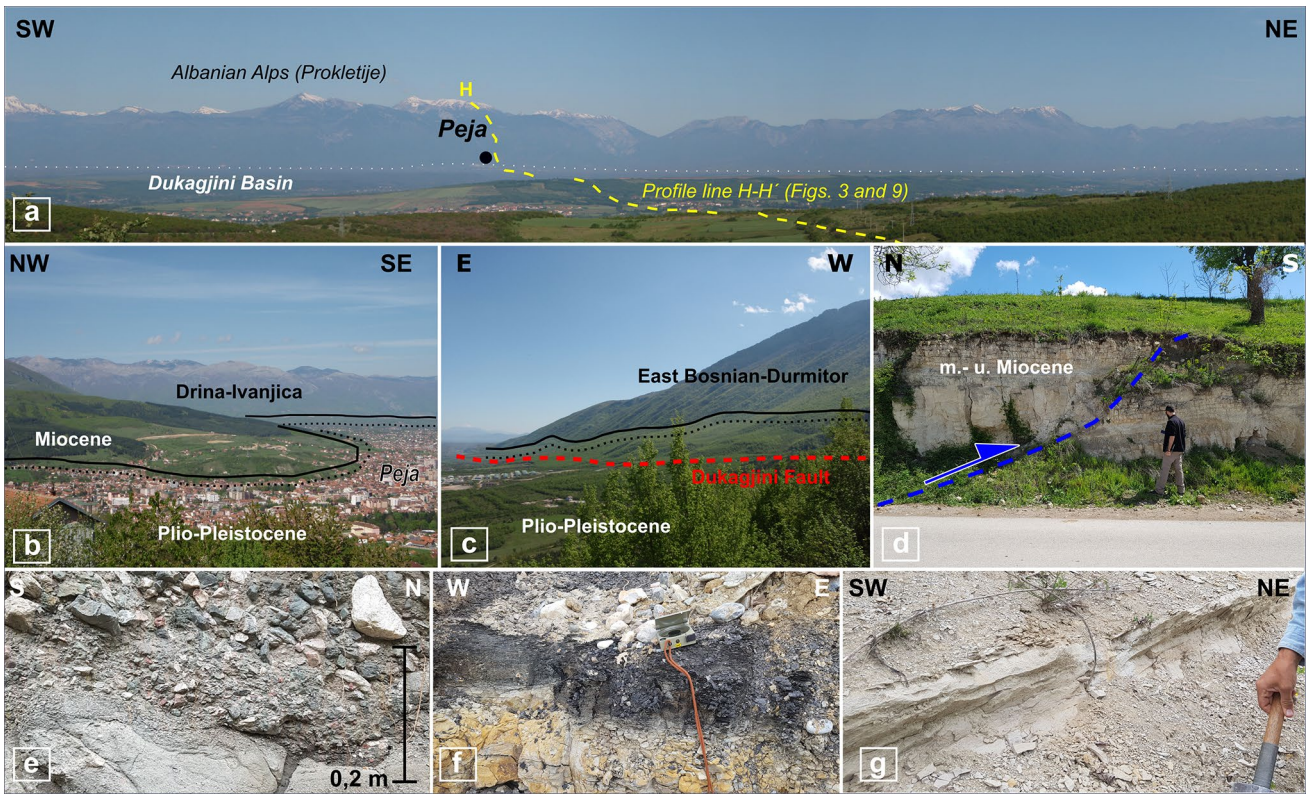

Fig. 8 Field impressions of the Dukagjini Basin: **a** Flat landscape and ~ 2500 m increase in relief along the SPNF; **b** Miocene sediments and unconformably overlying Plio-Pleistocene strata on which the city of Peja is built. In the background, Triassic limestone of the Drina–Ivanjica nappe forming the mountain range bounding the Dukagjini Basin to the north; **c** Plio-Pleistocene strata south of Peja that unconformably overlie the trace of Dukagjini Fault (dashed red line); **d** Thrusts in middle to upper Miocene sediments in the northeastern part of the Dukagjini Basin indicate N-S-directed shortening; **e** Poorly rounded and sorted basal conglomerate of middle Miocene age (~ 16 Ma) marking the onset of rift-related sedimentation in the Dukagjini Basin; **f** ~ 1 m thick layer of late Miocene lignite near Peja with calcareous-marly lacustrine strata above and below. Bedding of lignite layers dips 24° to the NW (348°); **g** Calcareous Pliocene (?) layer within shaley marl containing freshwater mollusks. Sediments dip 38° to the northwest (286°). Tilting of bedding is post-depositional

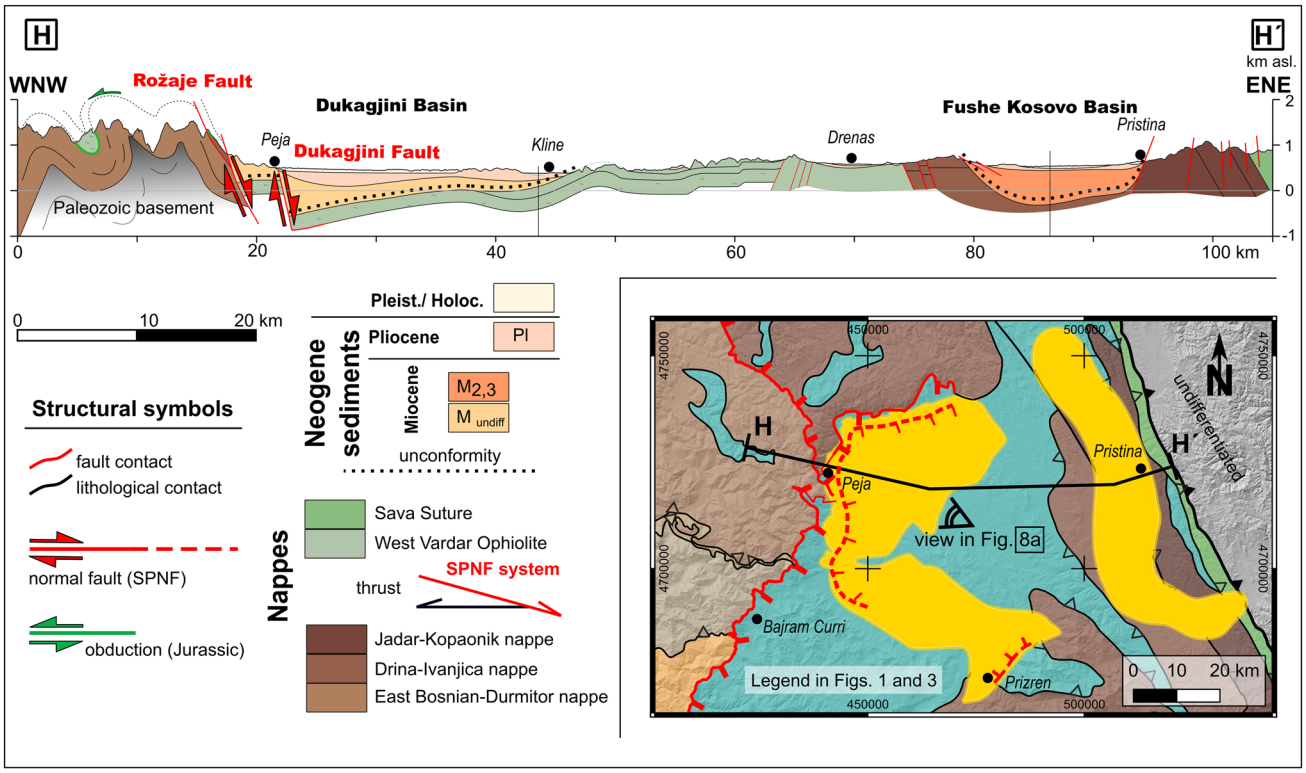

Fig. 9 Profile H–H' across the Dukagjini and Fushe Kosovo Basins in Kosovo (western part of profile trace in Fig. 3). Note the asymmetric, half-graben shape of the Dukagjini Basin. Vertical exaggeration is 3.5x. Legend for the nappes in inset map is shown in Figs. 1 and 3. Topographic profile and hillshade model extracted from ASTER GDEM (Abrams et al. 2020). Geology based on K34-53 "Pec", K34-65 "Kukes" (*Osnovna Geološka Karta SFRJ, 1:100.000* 1966–1977, Antonijević 1969) and Geological Map of Albania 1:200,000 and 1:50,000 (Xhomo et al. 2002). Structures and depth information are taken from the Tectonic Map of Kosovo 1:200,000, 2006 (Legler et al. 2006; Linder and Perkuhn 2013)

Ophiolite (Figs. 3 and 9, profile H–H´). The depth to the top of the basement (West Vardar Ophiolite) is indicated in Fig. 3 by dashed contour lines (Legler et al. 2006), revealing the crescent-like shape of the basin in map view that mimics both the arcuate traces of the Dukagjini Fault and the aforementioned segments of the SPNF (Knobloch et al. 2006; Legler et al. 2006). The deepest parts of the basin are 500 m below sea level and occur adjacent to the Dukagjini Fault, east and northeast of Peja (Figs. 3 and 10, Fig. 6 profiles E-E´, F-F´, G-G and I-I` and Fig. 9 profile H–H`). Borehole data (Elezaj 2009; Elezaj and Kodra 2012) indicate that the basin fill comprises Middle to Upper Miocene clastics (breccia, conglomerate, sandstone, lignite, Fig. 8) and lacustrine deposits (clay, lignite) that thicken towards the fault (Fig. 9, profile H–H') and are unconformably overlain by subhorizontal Plio-Pleistocene strata (Knobloch et al. 2006; Elezaj and Kodra 2012). This places a pre-Pliocene upper stratigraphic age limit on normal faulting along the Dukagjini Fault.

A throw of ~ 1000 m on the Dukagjini Fault in the western part of the DB (Figs. 3 and 6) is obtained from the difference between the basin surface and the depth of the unconformity at the base of the Miocene strata interpreted from the geoelectric data (contours in Figs. 3 and 6, profiles E-E´, F-F´, G-G; Fig. 9, profile H–H`). Between the Dukagjini and Rožaje Faults, Mid-Miocene sediments exposed at the surface lap onto the E-dipping West Vardar Ophiolite and its sub-ophiolitic mélange (Figs. 3, 8b, 8g). There, the basal Miocene unconformity dips gently towards the basin (Fig. 6, profile E-E`).

Along the northern margin of the DB in the hanging wall of the Dukagjini Fault, middle-to-upper Miocene sediments are locally affected by S-vergent thrusts (Fig. 8d), indicating that parts of the basin experienced post-late Miocene, N-S directed shortening.

Shkoder Klippe

The Shkoder Klippe (Figs. 2 and 3) lies ~ 75 km to the SW of the main West Vardar Ophiolite body of the internal Dinarides, but only a few km from a comparable body of West Vardar Ophiolite directly overlying the Krasta–Cukali Nappe of the northwestern Hellenides (Xhomo et al. 2002). The klippe is thus the most external

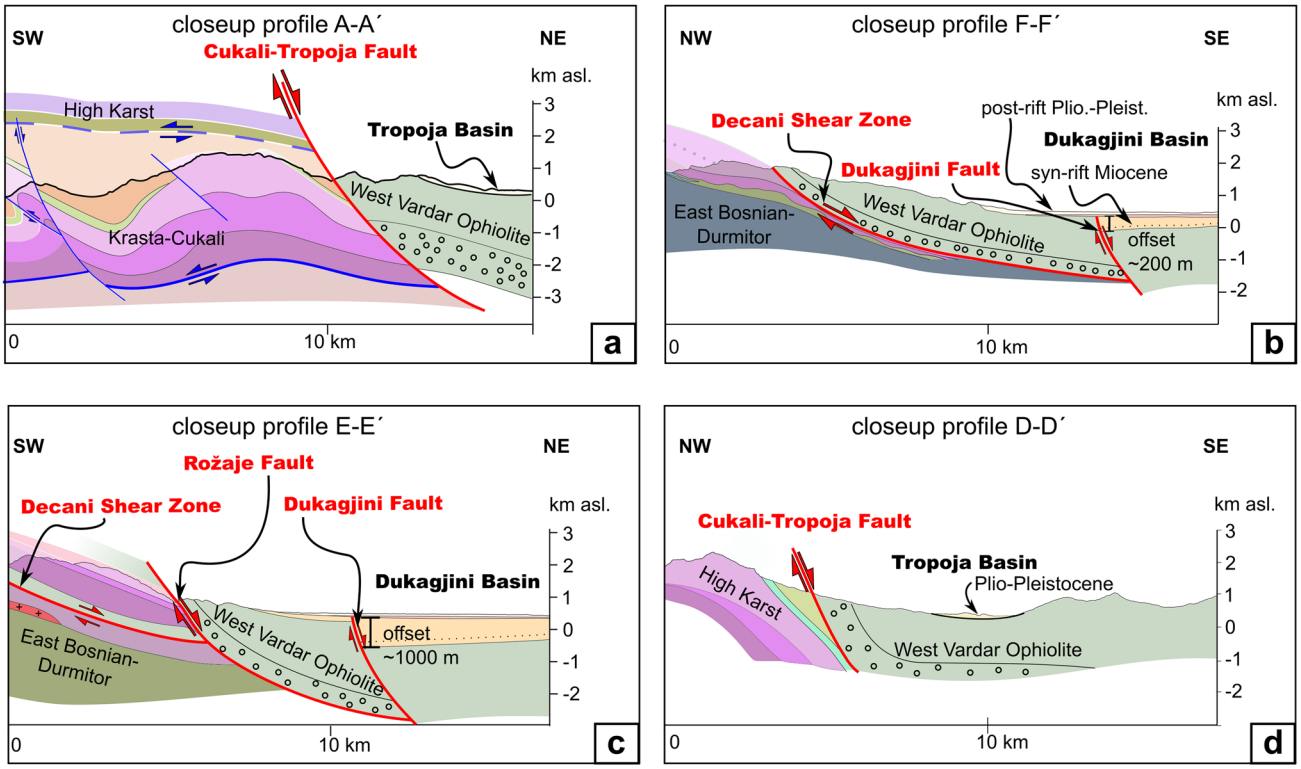

Fig. 10 Key parts of profiles in Figs. 4 and 6 that constrain the age of the SPNF system. Legend and traces of profiles shown in Fig. 3: **a** Cukali-Tropoja Fault cuts mid-Eocene to early Oligocene Dinaric thrusts and folds; **b** and **c** Decani Shear Zone cuts Dinaric folds and thrusts and thus is similarly young relative to doming and thrusting as the Cukali-Tropoja Fault. The Rožaje Fault cuts the Decani Shear Zone at depth and is thus younger. Both the Decani Shear Zone and Rožaje Fault are cut by the mid-Miocene Dukagjini Fault that borders the Dukagjini Basin. Post-rift Plio-Pleistocene sediments seal the Dukagjini Fault and unconformably overlie syn-rift Miocene sediments; **d** Plio-Pleistocene Tropoja Basin in the hanging wall of the Cukali-Tropoja Fault seal this fault segment

ophiolite body in the orogen and located immediately south of the NE-SW-trending offset marking the SPTZ.

Detailed mapping reveals that the obduction thrust overlying mélange within the klippe (obduction thrust marked violet in Fig. 2b) is truncated by a younger thrust that forms the base of the klippe and marks later, post-obduction emplacement of the klippe onto Paleogene flysch of the Krasta–Cukali nappe in the footwall of the SPNF (marked black in Fig. 2b). This basal thrust has top-W to -SW shear-sense indicators. The significance of this post-obduction thrust becomes evident when one considers that the Shkoder Klippe is located immediately to the north and west of the vertical rotation pole of the SPNF system marking the SW end of the Cukali–Tropoja fault. There, the West Vardar Ophiolite is not downthrown and no normal fault is observed. We, therefore, correlate the Shkoder Klippe with the large sheet of West Vardar Ophiolite overlying the Krasta–Cukali Nappe to the S and E along the northwestern Hellenides. Unfortunately, the Vau te Dejes reservoir lake (Figs. 2b and 3) obscures the lateral continuity of the klippe with the main West Vardar Ophiolite sheet to the SE.

We note that the basal thrust of the Shkoder Klippe is older than the base of the West Vardar Ophiolites immediately to the south, which was overprinted by Neogene thrusting related to clockwise rotation on the SPNF (Handy et al. 2019). In the next chapter, we discuss reasons supporting the idea that this basal thrust was active during dextral shearing along the SPTZ.

Age and kinematics of faulting, doming and basin formation

The cross-cutting relations of the segments of the SPNF (Fig. 10) and age of motions gleaned from structural relations, biostratigraphy and the few existing thermochronological data are summarized in Fig. 11.

Dextral motion on the Shkoder-Peja Transfer Zone (SPTZ)

The dextral offset of the front of the West Vardar Ophiolite by ~ 75 km along the SPTZ post-dates Early Cretaceous

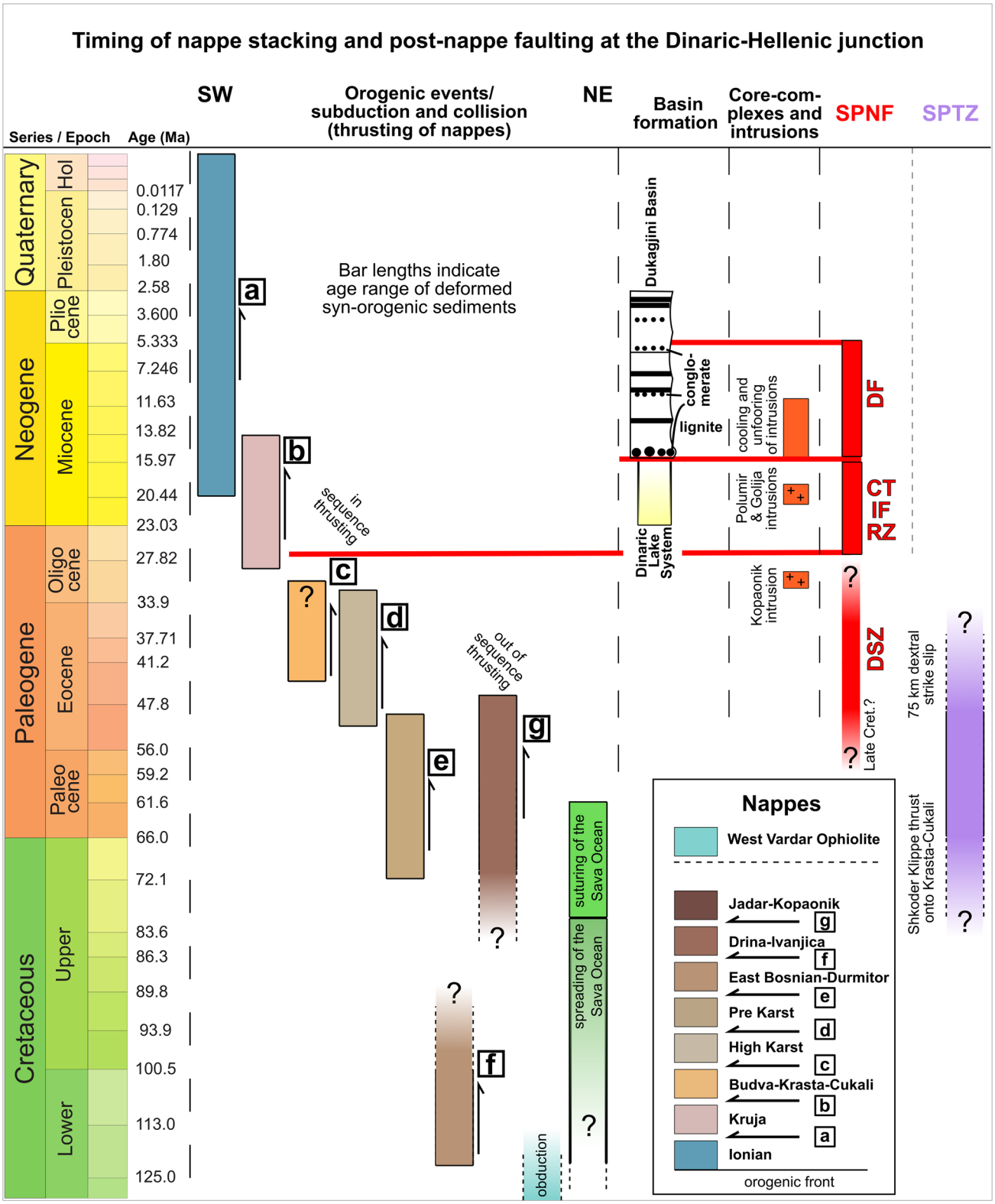

obduction of the West Vardar Ophiolite (Pamić 2002; Scherreiks et al. 2014; Tremblay et al. 2015) onto the undeformed Adriatic passive margin. An upper (younger) age limit on lateral motion of the SPTZ is given by the SPNF, which overprints the SPTZ and was not active as a normal fault before cessation of folding of the Dinaric nappe stack.

◂**Fig. 11** Ages of geological events at the Dinaric-Hellenic transition: Age of thrusting of Dinaric nappes, with bar lengths indicating the age range of deformed syn-orogenic sediments in the nappes and lowercase letters indicating time when nappe was emplaced onto next lower nappe according to stratigraphic ages in footwall of basal thrusts (Gorican 1994; Schmid et al. 2008, 2020; Mrinjek et al. 2012; Porkoláb et al. 2019; Cohen et al. 2013; van Hinsbergen et al. 2020; Balling et al. 2021). Sedimentation of Dukagjini Basin (Knobloch et al. 2006; Legler et al. 2006; Elezaj and Kodra 2012; Linder and Perkuhn 2013) and Dinaric Lake System (van Unen et al. 2019). Magmatism in the Kopaonik and Studenica core complexes (Schefer et al. 2011; Schefer 2012) and related core-complex formation and cooling. Activity of segments of the SPNF and the SPTZ as constrained by arguments in the text (Handy et al. 2019; Knobloch et al. 2006; Linder & Perkuhn 2013). Fault segments: *CT* Cukali–Tropoja Fault, *DSZ* Decani Shear Zone, *IF* Istog Fault, *RF* Rožaje Fault, *DF* Dukagjini Fault. It remains a matter of speculation whether or not 1st and 2nd phases of activity of the SPNF were distinct or continuous. See text regarding age of emplacement of the Shkoder Klippe

Tighter age constraints on the SPTZ come from the units that are not covered by the West Vardar Ophiolite. These are taken to define the minimum offset along the SPTZ, from the highest tectonic unit (Pre-Karst Nappe) beneath the West Vardar Ophiolite in the northeast (Fig. 3) to the Krasta–Cukali Nappe immediately underlying the basal thrust of the Shkoder Klippe near the proposed SW end of the SPTZ (Figs. 2b, 3 and 4a). At both localities, the flysch marking the youngest sediments in these nappes ranges in age from Late Cretaceous to Paleogene, i.e., Eocene (Gorican 1994; Dimitrijević 1997; Meço and Aliaj 2000) and even lower Oligocene if one takes into account clastic deposits further to the NW in the external Dinarides (e.g., Promina Beds in the High-Karst nappe (Mrinjek et al. 2012; Balling et al. 2021). These ages thus bracket the age of the SPTZ, with an Eo-Oligocene age dating the youngest possible age of nappe emplacement and offset. The SPTZ does not offset any of the more external Dinaric nappes with Oligocene flysch (Kruja, Ionian Nappes, Schmid et al. 2008 and refs therein), precluding a post-Oligocene age of dextral motion. The current orogenic front is also not dextrally offset, indicating that the SPTZ is no longer active.

A Paleogene age of dextral motion on the SPTZ can be deduced from map-scale kinematic reconstructions showing greater amounts of SW-directed Paleogene shortening in the Hellenides than in the Dinarides (van Hinsbergen et al. 2020). According to these authors, this differential shortening was related to closure of the Pindos Ocean in the Hellenides, a branch of Neotethys that was the along-strike equivalent of the Budva–Krasta–Cukali Basin in the Albanian part of the Hellenides and southern Dinarides. We speculate that the dextral offset on the SPTZ was kinematically linked with coeval SW-directed out-of-sequence thrusting and shortening in the Internal Dinarides (Fig. 11). If so, the amount of this shortening may be expected to be equivalent to the 75 km of dextral offset on the SPTZ. However, the amount and timing of this motion within the Late Cretaceous–Paleogene age range of motion are still unknown.

The question remains why a prominent fault like the SPTZ left no discernible traces in the field. A possible clue is that the basal thrusts of the external Dinaric nappes have undergone Mio-Pliocene reactivation (van Unen et al. 2019) and some may still active today (Bennett et al. 2008). Van Hinsbergen et al. (2020) estimate a minimum 30 km of thrusting of the High Karst Nappe onto the Krasta–Cukali Nappe in the last 5 Ma. This Plio-Pleistocene thrust is therefore younger than the dextral offset on the SPTZ. We propose that this young thrust buried the trace of the SPTZ, whose SW end must root in a part of the Krasta–Cukali Nappe beneath the High Karst Nappe, somewhere just to the north of the Shkoder Klippe, as depicted in Figs. 1 and 3. Higher units in the Dinaric nappe stack also preserve no traces of the SPTZ, ostensibly because they were deformed or eradicated by subsequent doming and normal faulting along the SPNF.

Shkoder-Peja normal faulting (SPNF)

We distinguish at least two phases of normal faulting along the SPNF: (1) an early phase of E-W to ESE-WNW directed mylonitic shearing along the Cukali–Tropoja Fault and Decani Shear Zone that syn- to post-dated footwall doming and post-nappe folding under greenschist-facies to anchizonal conditions. This metamorphism must be older than Eocene apatite fission-track ages ($T_{annealing}$ of 110–60 ℃, Gallagher et al. 1998; Reiners and Brandon 2006; Malusà and Fitzgerald 2018) from three samples, two of which are from the hanging wall of the Cukali-Tropoja Fault and one from the footwall of the Decani Shear Zone (Muceku et al. 2008, their Fig. 2). Though few in number and far apart, these ages suggest that there was little, if any normal displacement after thermal equilibration to 110–60 ℃ in Eocene time; (2) a later phase of ESE-WNW directed extensional faulting in Middle-to-Late Miocene time involved syn-rift sedimentation in the hanging wall of the Dukagjini Fault during tectonic subsidence of the Dukagjini Basin. The overprinting of calc-mylonite by cataclasite along the Cukali-Tropoja and Decani segments suggests that these two phases were discontinuous in time, with cataclasis affecting all segments of the SPNF, including the older Decani Shear Zone.

Pliocene (5.3 Ma) and younger sediments seal normal faults and mark the end of activity of the Dukagjini Fault bordering the Dukagjini Basin. An absolute younger stratigraphic age limit on the SPNF comes from horizontal Pleistocene–Holocene sediments in the northwestern part of the Tropoja Basin that seal the Cukali–Tropoja Fault (Fig. 10d, Gemignani et al. 2022, their Fig. 3). The Rožaje Fault segment cuts the unconformably overlying, tilted Miocene cover

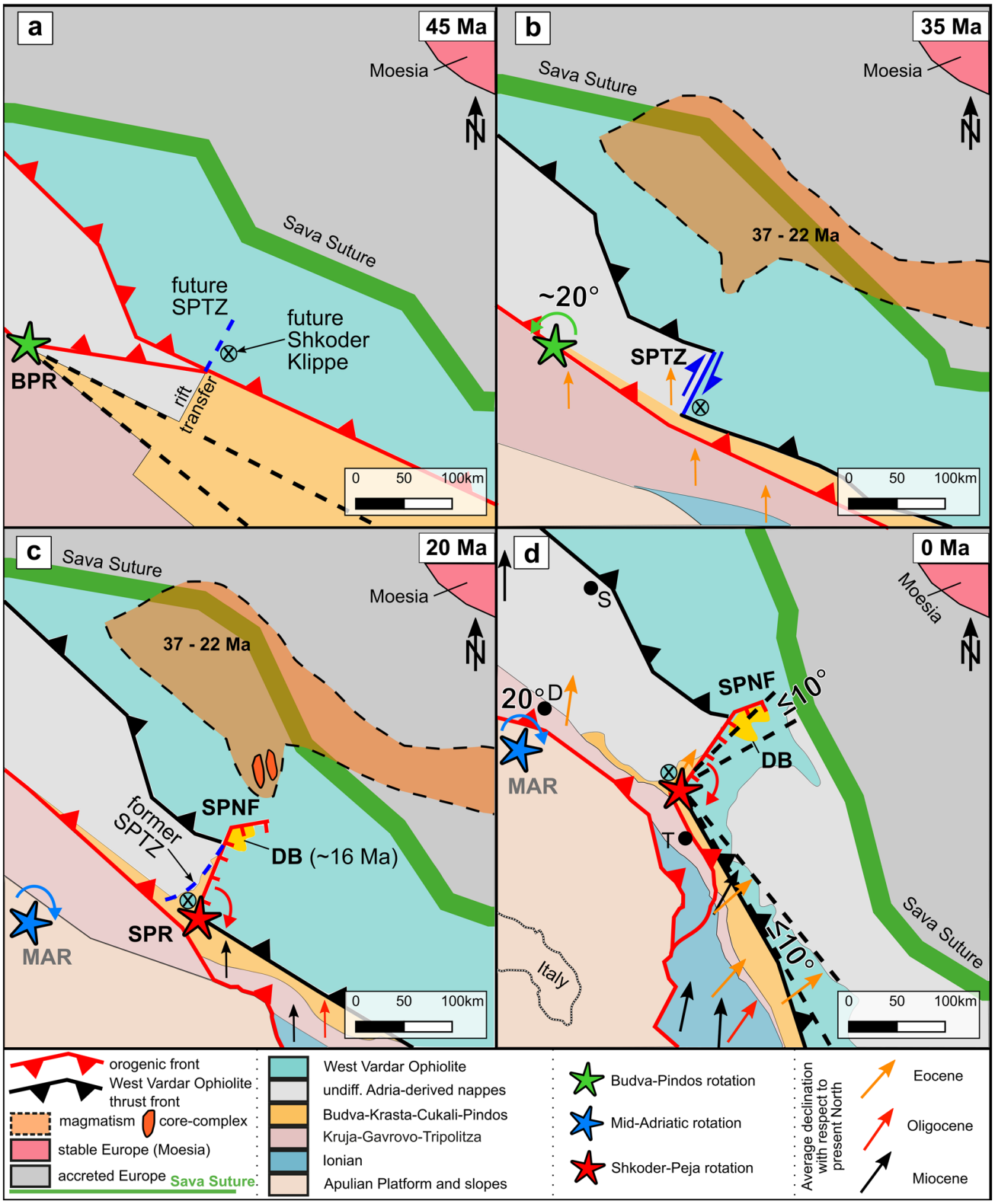

in its hanging wall near Peja (Figs. 3 and 6, profiles E-E` and G-G', Figs. 8f, g), indicating that it accommodated post-Miocene motion.

Model of orogen-parallel extension and orogenic arcuation

Figure 12 depicts the tectonics of the Dinaric–Hellenic

◂**Fig. 12** Kinematic evolution of the Dinaric–Hellenic Junction and associated fault structures from 45 Ma to Present: **a** At 45 Ma, onset of subduction of the Budva–Krasta–Cukali–Pindos Basin and Ocean around a counter-clockwise rotational axis (green star) marked BPR (Budva–Krasta–Cukali–Pindos). Dashed blue line marks the future SPTZ along a putative Mesozoic rift transfer fault transecting the Adriatic passive margin; **b** At 35 Ma, activity of the SPTZ has ceased after 75 km of dextral offset of the thrust front of the West Vardar Ophiolite. Magmatism, uplift and erosion begin to affect internal units of the Dinarides. The orogenic front has reached the base of the Krasta–Cukali Nappe. The SPNF nucleates along the SPTZ and accommodates SE-directed extension; **c** At 20 Ma, the second phase of extension on the SPNF (16 Ma-Present) is about to begin. Magmatism and extension occur along core complexes (orange). Extensional faulting involved a ~ 10° clockwise rotation of the Hellenides with respect to the Dinarides around a crustal rotational axis marked SPR (Shkoder-Peja rotation pole, red star). This entails the formation of the Dukagjini Basin (DB) in the hanging wall of the Dukagjini Fault. Orogenic bending of ~ 20° occurs about a lithospheric plate rotation pole marked MAR (Mid-Adriatic rotation pole, blue star). The orogenic front has reached the base of the Kruja Nappe; **d** Present-day situation with the SPNF separating oblique dextral collision in the SW-Dinarides from rollback subduction and clockwise rotation of the NW Hellenides. The orogenic front has reached the base of the Ionian Nappe. Apulian Platform and slope deposits generally after (Bernoulli 2001). Coloured arrows indicate average paleomagnetic declinations in variously aged sediments with respect to present north (see text for references). *Orange arrows* Eocene; *red arrows* Oligocene; *black arrows* Miocene (modified from Handy et al. 2019, their Fig. 11; after de Leeuw et al. 2012; Márton et al. 2003, 2014 and references therein). Cities: *T* Tirana; *D* Dubrovnik; *S* Sarajevo. Structures in all maps modified extensively from van Hinsbergen et al. (2020)

mountain belt at four critical time slices in the evolution of the junction based on the orogenic timetable in Fig. 11.

The paleotectonic map at 45 Ma (Fig. 12a) shows a scenario for the Adriatic passive margin and the advancing orogenic wedge at the latest possible onset of dextral shearing along the SPTZ. We propose that the SPTZ nucleated where the orogenic front impinged on a putative rift transfer that had formed during early Mesozoic rifting of Neotethys. Such transfer faults presumably accommodated the NW-to-SE increase in width of the Budva–Krasta–Cukali–Pindos domain (orange in Fig. 12a) which culminated in spreading of the Pindos Ocean in the SE (e.g., Schmid et al. 2021). Today, ophiolites derived from this branch of Neotethys are preserved in the Hellenides (Fig. 1a). The Budva part of this pelagic domain pinches out just to the NW of the SPTZ (Fig. 1b) and is proposed to be the potential site of a vertical rotation axis (green star labelled BPR in Fig. 12a) that accommodated Mesozoic opening and subsequent closure of the Budva–Krasta–Cukali–Pindos domain. The position of the leading edge of the West Vardar Ophiolite in Fig. 12a is speculative given the poor constraints on the amount and timing of NE-SW directed shortening on either side of the SPTZ. Nevertheless, this scenario is a kinematically viable explanation for localization of this fault. We emphasize that older (Late Cretaceous) motion on the SPTZ cannot be precluded given the broad stratigraphic constraints reviewed above.

By 35 Ma (Fig. 12b), dextral shearing on the SPTZ had probably ceased according to the stratigraphic age constraints in Fig. 11. The present dextral offset of the nappe stack between the Krasta–Cukali and Drina–Ivanjica Nappes (Figs. 1 and 2) is attributed to reactivation of the Early Mesozoic "transversale de Scutari-Peć" during Paleogene subduction and accretion of the Adriatic margin. Subduction of the Pindos Ocean has been inferred from Eo-Oligocene fore-arc turbidites in the Meso-Hellenic Basin (Figs. 1 and 12b, Ferrière et al. 2004). Subduction of the Budva–Krasta–Cukali–Pindos lithosphere in Paleogene time (e.g., Schmid et al. 2020) involved decreasing amounts of shortening from SE to NW along the chain (van Hinsbergen et al. 2020, their Figs. 36 and 37). This calls for counter-clockwise rotation of the Hellenic trench about the BPR axis during dextral strike-slip along the SPTZ (Fig. 12b). We note that the large dextral displacement along the SPTZ in Fig. 12b, which is basically constrained by today´s map-view offset of the West Vardar Ophiolite front (Fig. 1), differs from the lack of any offset in the reconstruction of van Hinsbergen et al. (2020, their Fig. 36) for their time slice at 30 Ma.

Calc-alkaline magmatism in Paleogene to Early Miocene (Schefer et al. 2011) time affected the upper plate of the Dinaric–Hellenic orogen, which lay well to the NE of the orogenic front and to the N and E of the SPTZ (Figs. 12b, c). This magmatism has been attributed to lithospheric delamination (Schefer et al. 2011) and/or subsequent detachment (breakoff, Andrić et al. 2018) of the Adriatic slab in response to a late Oligocene decrease in the Adria–Europe convergence rate (Handy et al. 2015). Indeed, delamination and/or slab detachment is a viable mechanism to explain two other striking features of the Dinaric orogen in latest Oligocene–Miocene time: first, the absence of Oligocene strata (Knobloch et al. 2006; Elezaj 2009; Meier 2012) beneath the Lower-to-Middle Miocene basal unconformity in the Dukagjini Basin (Figs. 6 and 8), and second, the formation of metamorphic core complexes in the vicinity of the Sava Suture (Bukulja, Kopaonik, Studenica, and Jastrebac core complexes in Figs. 1b, 12b; Marović et al. 2007; Schefer et al. 2011; Stojadinovic et al. 2013, 2016; Mladenović et al. 2015; Erak et al. 2016). We interpret both features as a manifestation of pre-Middle Miocene uplift and denudation of the upper plate associated with a period of enhanced slab retreat.

By 35 Ma (Fig. 12b), the SPNF had nucleated parallel to the older SPTZ. The early phase of extension on the SPNF (Cukali-Tropoja and Decani segments, possibly also Rožaje and Istog segments) post-dated SW-directed nappe thrusting and tight folding of the internal Dinaric nappes, but is difficult to place in a regional tectonic context due to the lack of tighter stratigraphic and thermochronological age

constraints. Late Cretaceous and/or Paleogene activity is possible, especially for the mylonitic Decani Shear Zone, as discussed in the previous section. We interpret early extension on the SPNF as a response to Paleogene delamination of the Adriatic slab beneath the Dinarides and Hellenides, as discussed above. Paleomagnetic declinations indicate incipient clockwise bending of the upper plate of the Adria–Europe subduction starting already in Eocene time and centred on a rotation axis at the Dinaric–Hellenic Junction (red star marked SPR in Figs. 12c). Rotation may have occurred in the wake of SW-ward retreat of the undetached part of the Adriatic slab beneath the Hellenides, as proposed by Handy et al. (2019). North of the SPNF, NE-SW directed orogen-normal extension is evidenced by Early to Middle Miocene half-grabens with extensive magmatism that young from NE to SW across the internal (Matenco and Radivojević 2012) and external Dinarides (Andrić et al. 2017; van Unen et al. 2019) towards the Dinaric foreland.

The Middle Miocene ushered in a change in the nature of crustal stretching, marked by the later phase of normal faulting along the SPNF (Fig. 12c). Whereas the early phase of extension along the SPNF was accompanied by exhumation, uplift and erosion, the later phase was marked by subsidence and basin filling. The Dukagjini Basin and others like it (e.g., Burrell and Librazhd Basins, Xhomo et al. 2002; NE end of the Meso-Hellenic Basin, Ferrière et al. 2004, Kallanxhi and Ćorić, 2017; locations in Figs. 1, 2 and 12c) are partly bounded by normal faults, which like the subsurface Dukagjini Fault, are all located in the hanging wall of the SPNF. Together, these normal faults accommodated coeval E-W and NW–SE extension (Handy et al. 2019). This biaxial extension has also been described in the central Southern Balkan region (central Albania and eastern Macedonia), which formed the upper plate of the retreating Hellenic orogen and subduction interface in Miocene time (Burchfiel et al. 2008). Subsequent subsidence and lacustrine deposition in Pliocene time outlasted Middle-to-Late Miocene normal faulting (Fig. 9, profile H–H´).

Post Middle–Late Miocene S-directed shortening in the Dukagjini Basin (Fig. 8d) corroborate fault-slip analyses indicating latest Miocene, NNE-SSW-directed shortening well to the north of the SPNF in the central Dinarides (van Unen et al. 2019). The causes of this shortening are debatable. Possibly, it is related to a short-lived increase in the rate of Adria–Europe convergence in latest Miocene time. This may have induced shortening that was transmitted across the orogenic front to the thinned upper plate in the Hellenides. However, this scenario remains speculative in the absence of studies on the areal extent of late shortening structures.

We now return to the question posed in the introduction regarding activity of the SPNF and its relationship to arcuation of the Dinarides and Hellenides. The kinematics of faulting at this junction require two, possibly three vertical rotation axes active at different times.

The first axis in Paleogene time at the NW end of the Budva–Krasta–Cukali–Pindos domain (green star marked BPR in Figs. 12a, b) is invoked on one hand to explain the NW-ward pinching out of this domain, and on the other hand, to account for differential subduction of this domain beneath the High-Karst, Pre-Karst and Pelagonian Nappes in the hanging wall of the orogenic front. The second axis affected only the orogenic crust and was located at the SW end of the SPNF at its basal décollement in the Krasta–Cukali Nappe (red star marked SPR in Figs. 12c, d), where Paleogene-to-Miocene extension increasing from 0 along the SPNF to the NE, met coeval shortening increasing to the SE along the Albanian Hellenides. (Handy et al. 2019). The third, more important rotation axis has been identified at or near the Mid-Adriatic Ridge (blue star marked MAR, Figs. 1, 12cd). This is the clockwise rotation pole for Miocene-to-recent segmentation of the Adriatic Plate into counter-rotating northern (counterclockwise) and southern (clockwise) subplates, respectively, named Adria sensu stricto (s.s.) and Apulia (Handy et al. 2019).

The rotation angles around the latter two vertical axes can be estimated from the amount of shortening and/or extension on the faults emanating from them. In the case of the Oligo-Miocene SPNF axis (Fig. 12c), an approximate clockwise angle of $\leq 10°$ is obtained by resolving the combined minimum vertical throws on the main segments of the SPNF (the Cukali-Tropoja and Dukagjini Faults) of ~ 3500 m at their NE ends onto their ~ 25° SE-ward dip to obtain a horizontal extension of ~ 7.5 km (Fig. 2a). We emphasize that locally steeper fault dips and greater throw along these segments of the SPNF yield, respectively, lesser and greater amounts of clockwise rotation about the SPNF axis. Away from the SPNF rotation pole to the NE, orogen-parallel extension is accommodated along an increasingly complex array of normal faults whose cumulate displacements are unaccounted for in our estimate.

Comparing the kinematically constrained rotations for the SPR and MAR axes with rotation estimates derived from paleomagnetic studies in the southern Dinarides and NW Hellenides lends insight into the timing, location and amount of orogenic arcuation in Paleogene-to Neogene time. In a compilation of published paleomagnetic data, Handy et al. (2019) showed that the Dinaric–Hellenic Orogen south of Dubrovnik (Fig. 1) has undergone ~ 50° of clockwise rotation relative to north since late Eocene time. This is indicated in Fig. 12d by orange arrows for the average paleo-declination directions in Eocene sediments on either side of the Dinaric–Hellenic Junction (refs. in caption). If taken at face value, the 50° of rotation exceeds the observed 30° clockwise bend of the Dinaric–Hellenic Orogen by some 20°. Possibly, this discrepancy can be

attributed to the aforementioned rotation about the BPR axis associated with differential Eocene subduction of the Budva–Krasta–Cukali–Pindos domain. We note that the 50° rotation is poorly constrained, with an uncertainty of some 20° in the paleomagnetically derived rotations (Kissel and Speranza 1995, Speranza et al. 1995, their Fig. 9). However, a BPR axis explains both the NW-ward disappearance of the Budva–Krasta–Cukali–Pindos units, as well as the along-strike shallowing of basinal facies in this unit.

Conclusions

Bending of the Dinaric–Hellenic Orogen involved two kinematically and temporally distinct structures: the Shkoder-Peja Transfer Zone (SPTZ) that effected ~ 75 km of dextral offset, and the Shkoder-Peja Normal Fault (SPNF). The SPNF is a composite structure comprising five fault segments that accommodated E- to SE-directed orogen-parallel extension and contributed to clockwise orogenic bending.

Although previous paleomagnetic studies already pointed to the Dinaric–Hellenic Junction as the locus of Cenozoic clockwise rotation of Adria with respect to Europe (van Hinsbergen et al. 2005; Kissel and Speranza 1995; Speranza et al. 1995), our field-based work provides a more differentiated view of motions which can be used to reconstruct the evolution of this crucial orogenic join.

The ~ 75 km dextral offset along the SPTZ is attributed to reactivation of an inherited Early Mesozoic rift transfer fault in the Adriatic margin during Eocene accretion and subduction of the Budva–Krasta–Cukali Basin and Pindos Ocean. The opening and closure of this ocean, an arm of Neotethys, involved a clockwise rotation about a vertical axis located at the NE of this basin (Figs. 12a, b). The initiation of this rotation may have been kinematically linked to the onset of back-arc extension and slab rollback in the southern Hellenides (Aegean) at 45 Ma (Brun et al. 2016). Today, the only vestige of thrusting related to the SPTZ is a small klippe of West Vardar Ophiolite that overlies the external Dinaric nappes near Shkoder (Figs. 2 and 4).

For the SPNF, we distinguish an early phase of ductile-to-brittle activity on four of the five fault segments (Cukali–Tropoja, Decani, Rožaje, Istog segments) in late Cretaceous–Paleogene time from a later brittle phase on the fifth segment (Dukagjini Fault) beginning in Mid-Miocene time and ending no later than the Early Pliocene (Figs. 3, 8, 9 and 11). Although these phases of normal faulting had the same kinematics, they were probably discontinuous in time, with older fault segments locally overprinted by brittle structures of the younger phase. Miocene extension appears to have migrated into the hanging wall of the four older fault segments and ended along the Dukagjini segment as well as along other faults bounding Neogene basins to the S and E where Pliocene extension has been assessed (e.g., Burrell and Librazhd Basins, and Peshkopie Window Fig. 2).

We relate the first phase of motion on the SPNF to Oligo-Miocene magmatism, crustal extension and uplift, as well as incipient clockwise rotation of the Hellenides with respect to the Dinarides. The second phase of motion in mid-to-late Miocene time was associated with formation of the Dukagjini Basin and clockwise rotation about an intracrustal axis located just E of Shkoder (Fig. 3).

Acknowledgements This study was financed by the German Research Foundation (DFG grants Gi 825/4-1, Ha 21/21-1 and Pl 534/3-1) and a grant from PROMOS (German Academic Exchange Program, DAAD). We thank many colleagues, especially Benjamin Schmitz, Peter Biermanns, Stefan Schmid, Kamil Ustaszewski, Zenun Elezaj and Sali Mulaj, for discussions in the field and thereafter. Eline Le Breton helped us use G-plates to export and process the model of van Hinbergen et al. (2002) as a base for the map reconstructions in Fig. 12. Finally, we acknowledge the work of BSc and MSc students in mapping classes in Albania since 2012, notably Sascha Zertani, Philip Groß, Lisa Kaatz, Leonardo Caprioli and Sebastian Cionoiu. GIS work and graphics were designed with open-source software *QGis* and *Inkscape*.

Funding Open Access funding enabled and organized by Projekt DEAL.

Data availability Please contact the first author for the data published in this publication.

Declarations

Conflict of interest None.

References

Abrams M, Crippen R, Fujisada H (2020) ASTER Global Digital Elevation Model (GDEM) and ASTER Global Water Body Dataset (ASTWBD). Remote Sens 12:1–12. https://doi.org/10.3390/rs12071156

Andrić N, Sant K, Matenco L et al (2017) The link between tectonics and sedimentation in asymmetric extensional basins: Inferences from the study of the Sarajevo-Zenica Basin. Mar Pet Geol 83:305–332. https://doi.org/10.1016/j.marpetgeo.2017.02.024

Antonijević R (1969) Geological Map of Jugoslavia. Belgrade Fed Geol Surv

Aubouin J, Dercourt J (1975) Les transversales dinariques deriventelles de paleofailles transformantes ? CR Acad Sc Paris 281:347–350

Babić L, Hochuli PA, Zupanic J (2002) The Jurassic ophiolitic mélange in the NE Dinarides : dating, internal structure and geotectonic implications. Eclogae Geol Helv 95:263–275. https://doi.org/10.5169/seals-168959

Bajraktar F, Pruthi V, Hajdari R et al (2010) History of Geoheritage Conservation in Kosovo. Schriftenr Der Dtsch Gesellschaft Für Geowissenschaften 66:107–107. https://doi.org/10.1127/sdgg/66/2010/107

Balling P, Tomljenović B, Schmid SM, Ustaszewski K (2021) Contrasting along-strike deformation styles in the central external Dinarides assessed by balanced cross-sections: implications for the tectonic evolution of its Paleogene flexural foreland basin system. Glob Planet Change. https://doi.org/10.1016/j.gloplacha.2021.103587

Bennett RA, Hreinsdóttir S, Buble G et al (2008) Eocene to present subduction of southern Adria mantle lithosphere beneath the Dinarides. Geology 36:3–6. https://doi.org/10.1130/G24136A.1

Bernoulli D (2001) Mesozoic-tertiary carbonate platforms, slopes and basins of the external Apennines and Sicily. Anat an Orogen Apennines Adjac Mediterr Basins. Springer, New York, pp 307–325. https://doi.org/10.1007/978-94-015-9829-3_18

Bestmann M, Kunze K, Matthews A (2000) Evolution of a calcite marble shear zone complex on Thassos Island, Greece: Microstructural and textural fabrics and their kinematic significance. J Struct Geol 22:1789–1807. https://doi.org/10.1016/S0191-8141(00)00112-7

Bijwaard H, Spakman W (2000) Non-linear global P-wave tomography by iterated linearized inversion. Geophys J Int 141:71–82

Borojević Šoštarić S, Palinkaš AL, Neubauer F et al (2014) The origin and age of the metamorphic sole from the Rogozna Mts., Western Vardar Belt: new evidence for the one-ocean model for the Balkan ophiolites. Lithos 192–195:39–55. https://doi.org/10.1016/j.lithos.2014.01.011

Bortolotti V, Chiari M, Kodra A et al (2004) New evidences for Triassic morb magmatism in the Northern Mirdita Zone ophiolites (Albania). Ofioliti 29:247–250. https://doi.org/10.4454/ofioliti.v29i2.217

Bortolotti V, Chiari M, Marroni M et al (2013) Geodynamic evolution of ophiolites from Albania and Greece (Dinaric-Hellenic belt): one, two, or more oceanic basins? Int J Earth Sci 102:783–811. https://doi.org/10.1007/s00531-012-0835-7

Brun JP, Faccenna C, Gueydan F et al (2016) The two-stage Aegean extension, from localized to distributed, a result of slab rollback acceleration. Can J Earth Sci 53:1142–1157. https://doi.org/10.1139/cjes-2015-0203

Burchfiel BC, Nakov R, Dumurdzanov N et al (2008) Evolution and dynamics of the Cenozoic tectonics of the South Balkan extensional system. Geosphere 4:919–938. https://doi.org/10.1130/GES00169.1

Carosi R, Cortesogno L, Gaggero L, Marroni M (1996) Geological and petrological features of the metamorphic sole from the Mirdita nappe, northern Albania. Ofioliti 21:21–40

Cohen KM, Finney SC, Gibbard PL, Fan JX (2013) The ICS International Chronostratigraphic Chart. Episodes 36:199–204. http://www.stratigraphy.org/ICSchart/ChronostratChart2023-04.pdf

Cvijić J (1901) Die dinarisch-albanesische Scharung. Sitzungsberichte der Kais Akad der Wissenschaften, Wien

D'Agostino N, Métois M, Koci R et al (2020) Active crustal deformation and rotations in the southwestern Balkans from continuous GPS measurements. Earth Planet Sci Lett. https://doi.org/10.1016/j.epsl.2020.116246

de Leeuw A, Mandic O, Krijgsman W et al (2012) Paleomagnetic and geochronologic constraints on the geodynamic evolution of the Central Dinarides. Tectonophysics 530–531:286–298. https://doi.org/10.1016/j.tecto.2012.01.004

Dimitrijević MD (1997) Geology of Yugoslavia Geological Institute GEMINI. Geological Special Publication, New York

Dimo-Lahitte A, Monie P, Vergely P (2001) Metamorphic soles from the Albanian ophiolites: petrology, 40Ar/39Ar geochronlogogy, and geodynamic evolution. Tectonics 20:78–96

Elezaj Z (2009) Cenozoic molasse basins in Kosovo and their geodynamic evolution. Muzeul Olteniei Craiova Oltenia Stud Şi Comunicări Ştiinţele Naturii 25:343–350

Elezaj Z, Kodra A (2012) Geology of Kosova, 1. Tekst Universitar, Pristina

Elsie R (2004) Historical dictionary of Kosova. Rowman & Littlefield Publishers Inc, Lanham

Erak D, Matenco L, Toljić M et al (2016) From nappe stacking to extensional detachments at the contact between the Carpathians and Dinarides—the Jastrebac Mountains of Central Serbia. Tectonophysics 710–711:162–183. https://doi.org/10.1016/j.tecto.2016.12.022

Ferriere J, Baumgartner PO, Chanier F (2016) The Maliac Ocean: the origin of the Tethyan Hellenic ophiolites. Int J Earth Sci 105:1941–1963. https://doi.org/10.1007/s00531-016-1303-6

Ferrière J, Reynaud J-Y, Pavlopoulos A et al (2004) Geologic evolution and geodynamic controls of the Tertiary intramontane piggyback Meso-Hellenic basin, Greece. Bull La Soc Geol Fr 175:361–381. https://doi.org/10.2113/175.4.361

Ferrill DA, Morris AP, Evans MA, Burkhard M, Groshong Jr. RH, Onasch CM (2004) Calcite twin morphology: a low-temperature deformation geothermometer. J Struct Geol 26:1521–1529

Gallagher K, Brown R, Johnson C (1998) Fission track analysis and its applications to geological problems. Annu Rev Earth Planet Sci 26:519–572. https://doi.org/10.1146/annurev.earth.26.1.519

Gawlick HJ, Frisch W, Hoxha L et al (2008) Mirdita Zone ophiolites and associated sediments in Albania reveal Neotethys Ocean origin. Int J Earth Sci 97:865–881. https://doi.org/10.1007/s00531-007-0193-z

Gemignani L, Mittelbach BV, Simon D et al (2022) Response of drainage pattern and basin evolution to tectonic and climatic changes along the Dinarides-Hellenides Orogen. Front Earth Sci 10:1–21. https://doi.org/10.3389/feart.2022.821707

Gorican S (1994) Jurassic and Cretaceous radiolarian biostratigraphy sedimentary evolution of the Budva Zone (Dinarides, Montenegro). Doctoral thesis, Mémoires de Géologie (Lausanne) No. 18. Universite de Lausanne, France

Groß P, Zertani S, Cionoiu S et al (2014) A new 1 : 10,000 geological map of the Skutari-Pec Fault and surroundings, northern Albania—evidence of orogen-parallel extension. Conference abstract for CBGA (Carpathian Balkan Geological Association), Tirana

Haas J, Jovanović D, Görög Á et al (2019) Upper Triassic-Middle Jurassic resedimented toe-of-slope and hemipelagic basin deposits in the Dinaridic Ophiolite Belt, Zlatar Mountain, SW Serbia. Facies 65:1–29. https://doi.org/10.1007/s10347-019-0566-3

Halamić J, Gorican S, Slovenec D, Kolar-Jurkovsek T (1999) A middle jurassic radiolarite-clastic succession from the medvednica Mt. (NW Croatia). Geol Croat 52:29–57. https://doi.org/10.4154/GC.1999.03

Handy MR, Giese J, Schmid SM et al (2019) Coupled crust-mantle response to slab tearing, bending and rollback along the Dinaride-Hellenide orogen. Tectonics. https://doi.org/10.1029/2019TC005524

Handy MR, Ustaszewski K, Kissling E (2015) Reconstructing the Alps–Carpathians–Dinarides as a key to understanding switches in subduction polarity, slab gaps and surface motion. Int J Earth Sci 104:1–26. https://doi.org/10.1007/s00531-014-1060-3

Hollenstein C, Müller MD, Geiger A, Kahle HG (2008) Crustal motion and deformation in Greece from a decade of GPS measurements,

1993–2003. Tectonophysics 449:17–40. https://doi.org/10.1016/j.tecto.2007.12.006
Kahle HG, Cocard M, Peter Y et al (2000) GPS-derived strain rate field within the boundary zones of the Eurasian, African, and Arabian Plates. J Geophys Res Solid Earth 105:23353–23370. https://doi.org/10.1029/2000jb900238
Kallanxhi M-E, Ćorić S (2017) Calcareous nannofossils from Oligocene-middle Miocene sediments from Albanian-Thessalian Basin (Albania): biostratigraphy and paleoecological implications. Conference: 16th International Nannoplankton Association Meeting, Athens, vol 37. https://www.researchgate.net/publication/320069101
Karamata S (2006) The geological development of the Balkan Peninsula related to the approach, collision and compression of Gondwanan and Eurasian units. Geol Soc Spec Publ 260:155–178. https://doi.org/10.1144/GSL.SP.2006.260.01.07
Kissel C, Speranza F, Milicevic V (1995) Paleomagnetism of external southern and central Dinarides and northern Albanides: implications for the Cenozoic activity of the Scutari-Pec Transverse Zone. J Geophys Res Solid Earth 100:14999–15007. https://doi.org/10.1029/95jb01243
Knobloch A, Legler C, Stanek KP, Dickmayer E (2006) Geological Map of Kosovo, 1:200,000. ICMM Kosova, Prishtina. Independent Commission for Mines and Minerals. https://www.kosovo-mining.org
Legler C, Stanek KP, Dickmayer E, Knobloch A (2006) Tectonic Map of Kosovo, 1:200,000. Independent Commission for Mines and Minerals, ICMM Kosova, Prishtina. https://www.kosovo-mining.org/
Liati A, Gebauer D, Fanning CM (2004) The age of ophiolitic rocks of the Hellenides (Vourinos, Pindos, Crete): first U-Pb ion microprobe (SHRIMP) zircon ages. Chem Geol 207:171–188. https://doi.org/10.1016/j.chemgeo.2004.02.010
Linder N, Perkuhn R (2013) Carbon Capture and Storage (CCS) in Kosovo. Fichtner Mining & Environment-Report for the World Bank, Essen. https://www.fichtner.de/en/projects/detailpage/carbon-capture-andstorage-ccs-capacity-building-in-kosovo
Louis H (1927) Albanien: Eine Landeskunde, vornehmlich auf Grund eigener Reisen. Geographische Abhandlungen- Verlag von J. Engelhorns Nachfolgern in Stuttgart, Berlin/Stuttgart
Lugović B, Slovenec D, Schuster R et al (2015) Petrology, geochemistry and tectono-magmatic affinity of gabbroic olistoliths from the ophiolite mélange in the NW Dinaric-Vardar ophiolite zone (Mts. Kalnik and Ivanščica, North Croatia). Geol Croat 68:25–49. https://doi.org/10.4154/gc.2015.03
Malusà MG, Fitzgerald PG (2018) Fission-Track thermochronology and its application to geology (Springer textbooks in earth sciences, geography and environment), 1st edn. Springer International Publishing, New York
Marović M, Djoković I, Toljić M et al (2007) Extensional unroofing of the Veliki Jastrebac dome (Serbia). Geol Anal Balk Poluostrva. 68:21–27. https://doi.org/10.2298/gabp0701021m
Marshak S (1988) Kinematics of orocline and arc formation in thin-skinned orogens. Tectonics 7:73–86
Márton E, Ćosović V, Moro A (2014) New stepping stones, Dugi otok and Vis islands, in the systematic paleomagnetic study of the Adriatic region and their significance in evaluations of existing tectonic models. Tectonophysics 611:141–154. https://doi.org/10.1016/j.tecto.2013.11.016
Márton E, Drobne K, Ćosović V, Moro A (2003) Palaeomagnetic evidence for Tertiary counterclockwise rotation of Adria. Tectonophysics 377:143–156. https://doi.org/10.1016/j.tecto.2003.08.022
Matenco L, Radivojević D (2012) On the formation and evolution of the Pannonian basin: constraints derived from the structure of the junction area between the Carpathians and Dinarides. Tectonics 31:1–31. https://doi.org/10.1029/2012TC003206
Meço S, Aliaj S (2000) Geology of Albania. Gebrueder Borntraeger. Berlin, Stuttgart
Meier J (2012) Die geologische Entwicklung des Prizren-Pejë-Beckens—The geological development of the Prizren-Pejë Basin. Zeitschrift für Geol Wissenschaften Berlin 40(1):35–42. http://www.zgwonline.de/en/media/035-121.pdf
Mladenović A, Trivić B, Cvetković V (2015) How tectonics controlled post-collisional magmatism within the Dinarides: Inferences based on study of tectono-magmatic events in the Kopaonik Mts. (Southern Serbia). Tectonophysics 646:36–49. https://doi.org/10.1016/j.tecto.2015.02.001
Mrinjek E, Nemec W, Pecinger V et al (2012) The eocene-oligocene promina beds of the Dinaric foreland basin in northern Dalmatia. J Alp Geol 55:409–451
Muceku B, Mascle GH, Tashko A (2006) First results of fission-track thermochronology in the Albanides. Geol Soc London, Spec Publ 260:539–556. https://doi.org/10.1144/gsl.sp.2006.260.01.23
Muceku B, Van Der Beek P, Bernet M et al (2008) Thermochronological evidence for Mio-Pliocene late orogenic extension in the north-eastern Albanides (Albania). Terra Nov 20:180–187. https://doi.org/10.1111/j.1365-3121.2008.00803.x
Neubauer TA, Harzhauser M, Georgopoulou E et al (2015) Tectonics, climate, and the rise and demise of continental aquatic species richness hotspots. Proc Natl Acad Sci U S A 112:11478–11483. https://doi.org/10.1073/pnas.1503992112
Okrusch M, Matthes S (2009) Mineralogie: Eine Einführung in die spezielle Mineralogie, Petrologie und Lagerstättenkunde, 8th edn. Springer, Berlin, Heidelberg
Osnovna Geološka Karta (SFRJ, 1:100.000, 1966–1977) Geozavod—OOUR Geoloski Institut Beograd 1966–1977—Socijalisticka Federativna Republika Jugoslavija
Ozsvárt P, Dosztály L, Migiros G et al (2012) New radiolarian biostratigraphic age constraints on Middle Triassic basalts and radiolarites from the Inner Hellenides (Northern Pindos and Othris Mountains, Northern Greece) and their implications for the geodynamic evolution of the early Mesozoic Neotet. Int J Earth Sci 101:1487–1501. https://doi.org/10.1007/s00531-010-0628-9
Pamić J (2002) The Sava-Vardar zone of the Dinarides and Hellenides versus the Vardar Ocean. Eclogae Geol Helv 95:99–114
Philpotts R, Ague JJ (2009) Principles of igneous and metamorphic petrology, 2nd edn. University Press, Cambridge
Porkoláb K, Kövér S, Benkó Z et al (2019) Structural and geochronological constraints from the Drina-Ivanjica thrust sheet (Western Serbia): implications for the Cretaceous-Paleogene tectonics of the Internal Dinarides. Swiss J Geosci 112:217–234. https://doi.org/10.1007/s00015-018-0327-2
Rassios AE, Dilek Y (2009) Rotational deformation in the Jurassic Mesohellenic ophiolites, Greece, and its tectonic significance. Lithos 108:207–223. https://doi.org/10.1016/j.lithos.2008.09.005
Reiners PW, Brandon MT (2006) Using thermochronology to understand orogenic erosion. Annu Rev Earth Planet Sci 34:419–466. https://doi.org/10.1146/annurev.earth.34.031405.125202
Robertson A, Karamata S, Šarić K (2009) Overview of ophiolites and related units in the Late Palaeozoic-Early Cenozoic magmatic and tectonic development of Tethys in the northern part of the Balkan region. Lithos 108:1–36. https://doi.org/10.1016/j.lithos.2008.09.007
Robertson A, Shallo M (2000) Mesozoic-Tertiary tectonic evolution of Albania in its regional Eastern Mediterranean context. Tectonophysics 316:197–254. https://doi.org/10.1016/S0040-1951(99)00262-0
Rosenbaum G (2014) Geodynamics of oroclinal bending: insights from the Mediterranean. J Geodyn 82:5–15. https://doi.org/10.1016/j.jog.2014.05.002

Rosenbaum G, Lister GS (2004) Formation of arcuate orogenic belts in the western Mediterranean region. Spec Pap Geol Soc Am 383:41–56. https://doi.org/10.1130/0-8137-2383-3(2004)383[41:FOAOBI]2.0.CO;2

Royden LH, Papanikolaou DJ (2011) Slab segmentation and late Cenozoic disruption of the Hellenic arc. Geochem Geophys Geosyst. https://doi.org/10.1029/2010GC003280

Schefer S (2012) Tectono-metamorphic and magmatic evolution of the Internal Dinarides (Kopaonik area, southern Serbia) and its significance for the geodynamic evolution of the Balkan Peninsula. Doctoral thesis, Philosophisch- Naturwissenschaftliche Fakultät der Universität Basel, Switzerland

Schefer S, Cvetković V, Fügenschuh B et al (2011) Cenozoic granitoids in the Dinarides of southern Serbia: age of intrusion, isotope geochemistry, exhumation history and significance for the geodynamic evolution of the Balkan Peninsula. Int J Earth Sci 100:1181–1206. https://doi.org/10.1007/s00531-010-0599-x

Scherreiks R, Meléndez G, BouDagher-Fadel M et al (2014) Stratigraphy and tectonics of a time-transgressive ophiolite obduction onto the eastern margin of the Pelagonian platform from late Bathonian until Valanginian time, exemplified in northern Evvoia, Greece. Int J Earth Sci 103:2191–2216. https://doi.org/10.1007/s00531-014-1036-3

Schmid SM, Bernoulli D, Fügenschuh B et al (2008) The Alpine-Carpathian-Dinaridic orogenic system: correlation and evolution of tectonic units. Swiss J Geosci 101:139–183. https://doi.org/10.1007/s00015-008-1247-3

Schmid SM, Fügenschuh B, Kounov A et al (2020) Tectonic units of the Alpine collision zone between Eastern Alps and western Turkey. Gondwana Res 78:308–374. https://doi.org/10.1016/j.gr.2019.07.005

Shallo M, Dilek Y (2007) Development of the ideas on the origin of Albanian ophiolites. In: Special Paper 373: Ophiolite concept and the evolution of geological thought. Geological Soc Am. 373:351–363

Speranza F, Islami I, Kissel C, Hyseni A (1995) Paleomagnetic evidence for Cenozoic clockwise rotation of the external Albanides. Earth Planet Sci Lett 129:121–134. https://doi.org/10.1016/0012-821X(94)00231-M

Stojadinovic U, Matenco L, Andriessen P et al (2016) Structure and provenance of Late Cretaceous-Miocene sediments located near the NE Dinarides margin: Inferences from kinematics of orogenic building and subsequent extensional collapse. Tectonophysics 710–711:184–204. https://doi.org/10.1016/j.tecto.2016.12.021

Stojadinovic U, Matenco L, Andriessen PAM et al (2013) The balance between orogenic building and subsequent extension during the tertiary evolution of the NE dinarides: Constraints from low-temperature thermochronology. Glob Planet Change 103:19–38. https://doi.org/10.1016/j.gloplacha.2012.08.004

Sudar M, Kovács S (2006) Metamorphosed and ductilely deformed conodonts from Triassic limestones situated beneath ophiolite complexes: Kopaonik Mountain (Serbia) and Bükk Mountains (NE Hungary)—a preliminary comparison. Geol Carpathica 57:157–176

Sudar MN, Gawlick HJ, Lein R et al (2013) Depositional environment, age and facies of the Middle Triassic Bulog and rid formations in the Inner Dinarides (Zlatibor Mountain, SW Serbia): Evidence for the Anisian break-up of the Neotethys Ocean. Neues Jahrb Fur Geol Und Palaontologie Abhandlungen 269:291–320. https://doi.org/10.1127/0077-7749/2013/0352

Tahirsylaj S, Kastrati B, Hasan H, Sopi F (2010) Hydro Geographical Elements of Bistrica E Pejes River. BALWOIS 2010—Ohrid. Repub Maced 25:1–4

Tari V (2002) Evolution of the northern and western Dinarides: a tectonostratigraphic approach. Stephan Mueller Spec Publ Ser 1:223–236. https://doi.org/10.5194/smsps-1-223-2002

Tremblay A, Meshi A, Deschamps T et al (2015) The Vardar zone as a suture for the Mirdita ophiolites, Albania: constraints from the structural analysis of the Korabi-Pelagonia zone. Tectonics 34:352–375. https://doi.org/10.1002/2014TC003807

van Hinsbergen DJJ, Langereis CG, Meulenkamp JE (2005) Revision of the timing, magnitude and distribution of Neogene rotations in the western Aegean region. Tectonophysics 396:1–34. https://doi.org/10.1016/j.tecto.2004.10.001

van Hinsbergen DJJ, Torsvik TH, Schmid SM et al (2020) Orogenic architecture of the Mediterranean region and kinematic reconstruction of its tectonic evolution since the Triassic. Gondwana Res 81:79–229. https://doi.org/10.1016/j.gr.2019.07.009

van Unen M, Matenco L, Nader FH et al (2019) Kinematics of Foreland-Vergent Crustal Accretion: inferences from the Dinarides evolution. Tectonics 38:49–76. https://doi.org/10.1029/2018TC005066

Vishnevskaya VS, Djeric N, Zakariadze GS (2009) New data on Mesozoic Radiolaria of Serbia and Bosnia, and implications for the age and evolution of oceanic volcanic rocks in the Central and Northern Balkans. Lithos 108:72–105. https://doi.org/10.1016/j.lithos.2008.10.015

von Nopcsa DBF (1905) Zur Geologie von Nordalbanien. Jahrb Der Kais Geol Reichsanstalt 55:85–152

Wortel MJR, Spakman W (2000) Subduction and slab detachment in the Mediterranean-Carpathian region. Sci Compass Rev 290:1910–1917. https://doi.org/10.1126/science.290.5498.1910

Xhomo A, Kodra A, Dimo-Lahitte A, Shallo M (2002) Geological Map of Albania 1:200.000—North. Repub Albania, Institute of Geological Researches, Oil and Gas Institute, FIER, Faculty of Geology and Mining, Albania